Stable isotopes of modern water across the Himalaya and eastern Tibetan Plateau: Implications for estimates of paleoelevation and paleoclimate

John Bershaw,[1] Sandra M. Penny,[2] and Carmala N. Garzione[1]

Received 21 April 2011; revised 21 November 2011; accepted 22 November 2011; published 27 January 2012.

[1] Paleoaltimetry based on stable isotopes ($\delta^{18}O$ and $\delta^{2}H$) of paleowater from the central and northern Tibetan Plateau is challenged by the lack of a clear relationship between isotopic composition and elevation north of the Himalaya. In order to determine the environmental factor(s) responsible for temporal changes in isotopic composition revealed in the geologic record, an understanding of the modern controls on isotope evolution in the continental interior is necessary. Here, we present new $\delta^{18}O$ and deuterium excess (*d excess*) data from modern surface water along a roughly south-north transect on the eastern part of the Himalaya and Tibetan Plateau. Results corroborate an inverse relationship between $\delta^{18}O$ and elevation in the Himalaya. Northward across the plateau, there is a positive trend in meteoric water $\delta^{18}O$ that is linear (~1.5‰ per degree latitude) and robust ($R^2 = 0.94$). A positive trend northward is also observed in *d excess* of surface water from large rivers. We show that Rayleigh distillation modified by surface water recycling can account for the observed spatial distribution of both $\delta^{18}O$ and *d excess* across the plateau. HYSPLIT modeling of air parcel back trajectories suggests that air mass mixing varies from east to west across the plateau. However, isotopic trends along the plateau's eastern margin are consistent with roughly parallel transects to the west, suggesting that a local process like moisture recycling exerts control over the isotopic evolution across the entire plateau, regardless of origin of air masses. Assuming the northern Tibetan Plateau was equally far from an oceanic source during late Eocene-Miocene time, paleoelevations of the Hoh Xil Basin are recalculated to account for recycling, increasing elevation estimates by 1100–2700 m.

Citation: Bershaw, J., S. M. Penny, and C. N. Garzione (2012), Stable isotopes of modern water across the Himalaya and eastern Tibetan Plateau: Implications for estimates of paleoelevation and paleoclimate, *J. Geophys. Res.*, *117*, D02110, doi:10.1029/2011JD016132.

1. Introduction

[2] Comparisons between stable isotopes of modern and paleo-waters ($\delta^{18}O$ and $\delta^{2}H$) have been used extensively to constrain temporal changes in surface elevation and climate [*Garzione et al.*, 2000b; *Poage and Chamberlain*, 2001; *Rowley et al.*, 2001; *Garzione et al.*, 2006; *Quade et al.*, 2007; *Saylor et al.*, 2009; *Mulch et al.*, 2010]. This technique requires knowledge of how isotopes of precipitation change with elevation, which is well-defined on the windward side of many mountain ranges [*Poage and Chamberlain*, 2001] including the Himalaya [*Garzione et al.*, 2000a; *Karim and Veizer*, 2002; *Hren et al.*, 2009]. Using the modern isotopic lapse rate, $\delta^{18}O$ values from carbonates in the Himalaya suggest it attained its current elevation by the late Miocene [*Garzione et al.*, 2000b, 2000a; *Rowley et al.*, 2001; *Saylor et al.*, 2009]. The timing of surface uplift across the Tibetan Plateau, north of the Himalaya, has proved more difficult to constrain as there is not a clear relationship between elevation and isotopes of precipitation across the Plateau [*Quade et al.*, 2007, 2011]. Factors other than elevation may significantly affect isotopes of precipitation north of the Himalayan crest including evaporation under arid conditions, recycling of surface water, and changes in the relative influence of moisture sources [*Numaguti*, 1999; *Tian et al.*, 2001; *Yamada and Uyeda*, 2006; *Kurita and Yamada*, 2008; *Hren et al.*, 2009]. When and how surface uplift occurred across Tibet is still relatively ambiguous due to the difficulty in interpreting isotopes of both modern and paleo-water, in addition to a paucity of data from the central to northern plateau [*Molnar et al.*, 2010].

[3] Isotopes of modern meteoric water have been used to constrain the spatial extent and magnitude of Asian monsoon influence (both Indian and East Asian) on precipitation across the Tibetan Plateau [*Araguás-Araguás et al.*, 1998; *Tian et al.*, 2001; *Vuille et al.*, 2005; *Joswiak et al.*, 2010],

[1]Department of Earth and Environmental Sciences, University of Rochester, Rochester, New York, USA.
[2]Department of Atmospheric Sciences, University of Washington, Seattle, Washington, USA.

Copyright 2012 by the American Geophysical Union.
0148-0227/12/2011JD016132

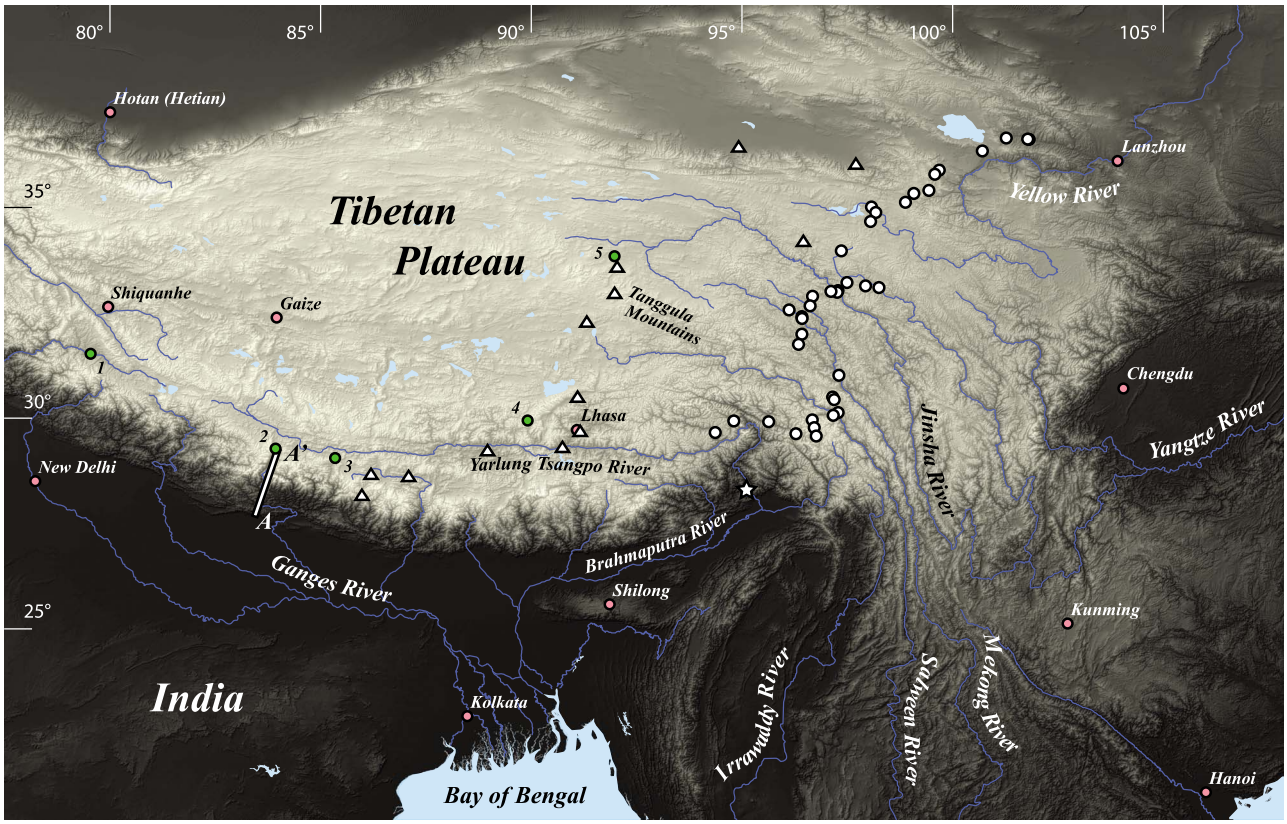

Figure 1. Sample location map of surface water collected across the eastern Tibetan Plateau (white open circles). Locations also shown for other published data sets discussed in the text including river waters across the central Tibetan Plateau (white open triangles) [*Tian et al.*, 2001], central Himalayan tributaries along transect A-A′ [*Garzione et al.*, 2000a], and low elevation tributaries of the Brahmaputra (open star) [*Hren et al.*, 2009]. *Yu et al.* [2007] include precipitation data across the western plateau from New Delhi, Shiquanhe, Gaize, and Hotan. GNIP (Global Network of Isotopes in Precipitation) place names shown as pink circles. Paleoaltimetry studies mentioned in the text are shown as green circles. One is the location of *Saylor et al.*'s [2009] study, 2 is for *Garzione et al.* [2000a; 2000b], 3 is for *Rowley et al.* [2001], 4 is for *Spicer et al.* [2003], and 5 is for *Cyr et al.* [2005] and *Polissar et al.* [2009]. Shaded relief topography derived from satellite data (SRTM from http://srtm.csi.cgiar.org).

although it is still not clear how temporal changes in meteoric water δ^{18}O are related to the monsoon [*Dayem et al.*, 2010]. Though variation in monsoon strength has been related to the height and/or extent of both the Himalaya and the Tibetan Plateau [*Kutzbach et al.*, 1993; *An et al.*, 2001], the role topography plays in the timing and intensity of the Asian monsoon is debated [*Boos and Kuang*, 2010]. A better understanding of the monsoon's contribution to precipitation across the Tibetan Plateau (and vice versa) is not only important for research on climate and elevation histories of Asia, but for accurate predictions of climate change's effect on the Asian monsoon [*Thompson et al.*, 2000]. This is especially relevant for the billions of people that depend on monsoon rains to sustain agriculture and their economy [*Tao et al.*, 2004; *Gadgil and Rupa Kumar*, 2006].

[4] Here, we present new stable isotope data (δ^{18}O and δ^{2}H) from modern surface waters collected on a south-north transect along the eastern margin of the Tibetan Plateau (Figure 1). Results show an inverse relationship between δ^{18}O and deuterium excess (*d excess*) up the windward side of the Himalaya and increase in both δ^{18}O and *d excess* northward across the plateau. Results are consistent with published isotopic and climate data from surrounding areas [*Garzione et al.*, 2000a; *Tian et al.*, 2001; *Karim and Veizer*, 2002; *Hren et al.*, 2009; IAEA/WMO, Global Network of Isotopes in Precipitation, 2010, http://www-naweb.iaea.org/napc/ih/IHS_resources_gnip.html]. We use a Rayleigh model of vapor distillation modified by evaporation at low relative humidity to evaluate whether recycling can explain observed trends in δ^{18}O and *d excess*. Isotopic results are also considered in the context of Hybrid Single-Particle Lagrangian Integrated Trajectory (HYSPLIT) modeling of regional air mass movement [*Draxler and Hess*, 1998; R. Draxler and G. Rolph, HYSPLIT (HYbrid Single-Particle Lagrangian Integrated Trajectory) Model, 2010, access via NOAA ARL READY Web site: http://ready.arl.noaa.gov/HYSPLIT.php] to evaluate the relative contribution of unique moisture sources to precipitation. Consistent trends in δ^{18}O and *d excess* across the plateau, regardless of changes in source from east to west, suggest that continental recycling overprints original isotopic signals on the northern plateau. This means that temporal changes in the balance of moisture source contribution to plateau precipitation may not have as

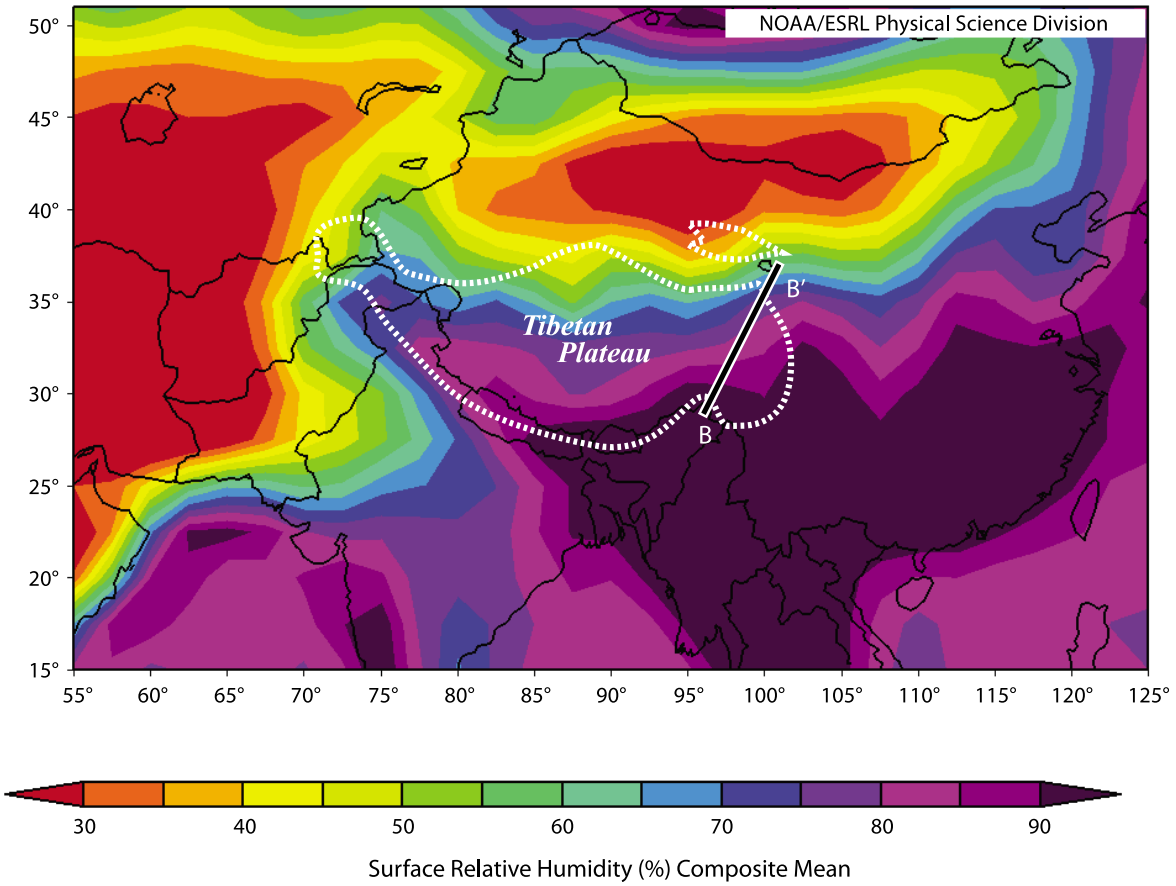

Figure 2. Composite of NCEP/NCAR reanalysis data showing average relative humidity at the land/sea surface for summer months (JJA) from 1948 to 2010. Transect B-B′ is approximate location of surface water samples collected for this study. Dashed white curve is a smoothed 4000 m elevation contour showing rough outline of the Tibetan Plateau. Image provided by the NOAA/ESRL Physical Sciences Division, Boulder Colorado from their Web site at http://www.esrl.noaa.gov/psd [*Kalnay et al.*, 1996].

profound an effect on the isotopic composition of paleowaters as recycling within this deeply continental setting.

2. Climate

[5] As the highest and most extensive topographic feature on Earth, the Tibetan Plateau significantly affects atmospheric circulation on a regional, and even global scale [*Yanai and Wu*, 2006; *Wen et al.*, 2010]. Weather station data indicates that the majority of precipitation falls during the summer months (auxiliary material Figure S1) (IAEA/WMO Web site, 2010) and is the result of both synoptic (plateau) scale and local disturbances [*Ueno et al.*, 2001; *Yamada and Uyeda*, 2006].[1] Though less in amount, there is also significant precipitation at high elevations in the Himalaya during winter months [*Tian et al.*, 2005]. On the Tibetan Plateau, evaporation of surface waters and falling raindrops in the air column is significant [*Yamada and Uyeda*, 2006; *Kurita and Yamada*, 2008]. During summer months (JJA), average relative humidity on the plateau surface decreases from ~85% in the south to ~60% in the north (Figure 2). The plateau also becomes more isolated from ocean basins northward which results in an increase in the relative contribution of recycled moisture from continental sources to the north.

[6] Precipitation on the plateau may be derived from multiple sources including the Indian Ocean (Indian Monsoon), the Pacific (Southeast Asian Monsoon), the Arctic (northerlies), the Atlantic (westerlies), continental lakes, and/or soil water. The Indian monsoon provides the majority of summer precipitation to the southern Himalaya and transports vapor onto the plateau through deeply incised river valleys like the Brahmaputra and Kali Gandaki [*Garzione et al.*, 2000a; *Hren et al.*, 2009]. A transition from Indian monsoon to continental (westerly and/or northerly) moisture sources northward across the plateau has been inferred from the isotopic composition of rainfall and surface waters [*Araguás-Araguás et al.*, 1998; *Tian et al.*, 2001; *Joswiak et al.*, 2010]. In addition to a latitudinal change in moisture source affinity, an altitudinal distinction has been suggested between continental (westerly or northerly)

[1]Auxiliary materials are available in the HTML. doi:10.1029/2011JD016132.

derived air masses dominating high elevation precipitation (snow) in the Himalaya and Indian monsoonal (southerly) air masses dominating relatively low elevation precipitation in the Himalayan foreland and up longitudinal valleys in southern Tibet [*Tian et al.*, 2005; *Barros et al.*, 2006]. This study presents isotopic results from the plateau's eastern margin which is both closer to the Pacific Ocean and deeply incised by major transverse rivers draining southeastward off the plateau (Figure 1).

2.1. Oxygen and Hydrogen Isotopes of Surface Water

[7] River and stream water may consist of precipitation and/or groundwater, depending on the amount of recent rainfall and size of the catchment. Smaller catchments will be more affected by recent precipitation events than large rivers [*Salati et al.*, 1979]. Though there is uncertainty in the spatial and temporal distribution of precipitation represented in river water, its tendency to integrate precipitation makes it a better representation of monthly or annual weighted averages than individual precipitation events [*Kendall and Coplen*, 2001]. In the absence of long-term precipitation records, we compare modern river water to geologic proxies for paleowaters which tend to integrate the isotopic composition of surface water over both space and time [*Gile et al.*, 1966; *Breecker et al.*, 2009].

[8] A definable relationship between elevation and the isotopic composition of meteoric water ($\delta^{18}O$ and $\delta^{2}H$) exists on the windward side of the Himalaya, conforming to a simple Rayleigh distillation model of air mass depletion [*Quade et al.*, 2007; *Rowley and Garzione*, 2007]. This relationship is attenuated by subcloud and surface water evaporation on the Tibetan Plateau which lies in the Himalayan rainshadow [*Tsujimura et al.*, 2001; *Gat and Airey*, 2006; *Yamada and Uyeda*, 2006; *Yang et al.*, 2007a]. Variability in the relative contribution of unique moisture sources to precipitation across the Tibetan Plateau may also affect $\delta^{18}O$ and $\delta^{2}H$ values [*Araguás-Araguás et al.*, 1998; *Tian et al.*, 2001; *Yang et al.*, 2006; *Yu et al.*, 2007; *Joswiak et al.*, 2010]. Thus, temporal shifts in the isotopic composition of paleowaters preserved in the geologic record may be related to changes in a region's topography, climate, and/or source(s) of moisture [*Chamberlain and Poage*, 2000; *Garzione et al.*, 2000a; *Graham et al.*, 2005; *Kent-Corson et al.*, 2009].

[9] A deuterium excess (*d excess*) in water results from fractionation of isotopes during phase changes due to vapor pressure differences among H_2O molecule isotopologues and differences in diffusion rates among isotopologues where relative humidity <100% [*Stewart*, 1975; *Froehlich et al.*, 2002]. Deuterium excess (*d excess*) was defined by *Dansgaard* [1964] as a function of deuterium (^{2}H) and heavy oxygen (^{18}O) in water:

$$d\ excess = \delta^{2}H_{w} - 8 * \delta^{18}O_{w}. \quad (1)$$

[10] The global average *d excess* in precipitation was found to be about 10‰. Vapor derived from the eastern Mediterranean Sea is known to have significantly higher *d excess* values (~20‰) compared to vapor derived from the Indian or Pacific Oceans (~10‰) [*Gat and Carmi*, 1970]. For the Himalaya and Tibetan Plateau, relatively high *d excess* values in meteoric water have been used to infer Mediterranean or westerly derived vapor [*Karim and Veizer*, 2002; *Tian et al.*, 2005, 2007; *Hren et al.*, 2009]. However, *d excess* values have also been shown to vary significantly based on local environmental conditions, such as the temperature of condensation, amount of subcloud evaporation during rainout, and degree of local moisture recycling [*Jouzel and Merlivat*, 1984; *Gat and Airey*, 2006; *Liotta et al.*, 2006; *Froehlich et al.*, 2008; *Kurita and Yamada*, 2008; *Cui et al.*, 2009].

2.2. Paleoclimate, Paleoelevation, and Paleogeography

[11] High topography in the Himalaya was likely generated soon after the initiation of Indo-Eurasian convergence ~45–55 Ma [*Rowley*, 1996; *Searle et al.*, 1997; *Zhu et al.*, 2005]. Stable isotopes ($\delta^{18}O$ and $\delta^{13}C$) of sedimentary carbonates, speleothems, fossil teeth, and fresh-water bivalves have all been used to constrain the isotopic evolution of paleowaters throughout Asia. In the Himalaya and southernmost Tibet, south of the Indus-Tsangpo suture, sedimentary carbonates suggest current elevations were attained by the late Miocene [*Garzione et al.*, 2000b, 2000a; *Rowley et al.*, 2001; *Saylor et al.*, 2009] (Figure 1). Paleotemperatures from fossil leaves also indicate southern Tibet, north of the Indus-Tsangpo suture, has been high since at least ~15 Ma [*Spicer et al.*, 2003].

[12] Ranges on the northern and northeastern Tibetan Plateau were likely elevated by the Eocene or latest Oligocene considering that crustal shortening and basin development were well underway along the Altyn Tagh fault [*Yin et al.*, 2002; *Ritts et al.*, 2004] and in the Hoh Xil, Qaidam, and Minhe-Xining Basins [*Horton et al.*, 2004; *Zhou et al.*, 2006; *Zhu et al.*, 2006; *Yin et al.*, 2008]. The presence of high topography on the northeast margin of the Tibetan Plateau by the late Eocene is also inferred from pollen in lacustrine sediments [*Dupont-Nivet et al.*, 2008]. Stable isotopes from the Tarim and Qaidam basins along the plateau's northern margin also suggest significant topography existed in basin-bounding ranges by the end of the Paleogene [*Kent-Corson et al.*, 2009]. In the central and northern Tibetan Plateau, isotope records are interpreted with less certainty as factors other than elevation significantly affect modern meteoric water $\delta^{18}O$ and $\delta^{2}H$ values [*Tian et al.*, 2001; *Quade et al.*, 2007; *Yu et al.*, 2008; *Molnar et al.*, 2010]. Because it can be difficult to distinguish between temporal changes in climate and/or elevation as the forcing behind shifts in isotope records, it is helpful to consider isotopes in the context of other proxies.

[13] Arid conditions in the Asian continental interior could have been caused by surface uplift of surrounding ranges, global cooling, the retreat of an epicontinental sea (Paratethys), and/or meridional plate drift into relatively dry, subtropical latitudes. Eolian deposits throughout China have been interpreted to result from cooling and drying of the Asian interior [*An et al.*, 2001; *Guo et al.*, 2002; *Sun et al.*, 2010]. On the western loess plateau, *Garzione et al.* [2005] documented earliest loess deposition to ~29 Ma, not long after playa deposits become prominent in northeastern Tibet ~34 Ma [*Dupont-Nivet et al.*, 2007]. This may post-date retreat of an epicontinental sea (Paratethys) from the western Tarim Basin in the late Eocene [*Bosboom et al.*, 2010], though marine sedimentary rocks have been documented in the Qaidam Basin as late as the middle Miocene [*Ritts et al.*,

Table 1. Catchment Size, Locality Information, and Stable Isotope Results for Surface Water and Snow Across the Tibetan Plateau

Sample Identification	$\delta^{18}O$ (VSMOW)	$\delta^{2}H$ (VSMOW)	*d excess*	Elevation (m)	Latitude	Longitude	Catchment Size (km^2)	Latitude (Centroid)[a]	Longitude (Centroid)[a]
				Streams and Rivers					
JBTB-01	−7.8	−46	16.2	2216	36.6193	101.8078	36193.6	37.1993	100.0424
JBTB-02	−7.6	−47.9	12.6	2245	36.6277	101.7744	399.3	36.4535	101.6138
JBTB-03	−8.3	−53.4	12.6	2669	36.6501	101.2667	606.3	36.4929	101.1844
JBTB-04	−8.4	−58.3	8.7	3070	36.3514	100.7023	38.2	36.4055	100.6843
JBTB-06	−9.1	−59.7	13.2	3749	35.8876	99.6758	206.2	35.9558	99.5644
JBTB-07	−10.2	−69.1	12.7	3724	35.7898	99.5697	1489.4	35.9196	99.3017
JBTB-08	−10.9	−70.5	16.6	3932	35.4078	99.4303	56.6	35.4687	99.4275
JBTB-09	−12.1	−84.9	11.7	4134	35.3349	99.0719	50.3	35.3814	99.0655
JBTB-10	−12	−81.9	13.9	4212	35.1271	98.8749	747.1	34.9367	98.9285
JBTB-12	−11	−82.2	5.7	4235	35.0131	98.0687	501	35.0692	98.2243
JBTB-16	−10.4	−76.9	6	4216	34.6709	98.0459	1255.3	34.4895	97.7968
JBTB-20	−11.5	−82.2	9.9	4515	33.9708	97.3515	641.8	34.0233	97.5383
JBTB-23	−13	−93.2	10.6	4366	33.2214	97.4858	28.9	33.1995	97.4969
JBTB-25	−13.7	−98.7	11	3994	33.1013	98.2447	14434.3	33.4954	97.7523
JBTB-26	−13.8	−99	11.5	4101	33.1401	97.9256	1265.7	33.0901	97.7101
JBTB-28	−14	−99.1	12.5	3625	33.0303	97.2709	438.4	33.1228	97.384
JBTB-29	−11.9	−83	12.2	3529	32.9891	97.2527	238597.4	34.4763	91.6872
JBTB-31	−14.9	−105.6	13.6	3629	33.0104	97.1061	2389.2	32.8572	96.9933
JBTB-34	−13.7	−97.7	12	4368	32.896	96.6689	9.9	32.8825	96.6859
JBTB-35	−15.4	−110	12.9	3952	32.6689	96.6121	703.1	32.7865	96.698
JBTB-36	−14.6	−104.9	12.2	3783	32.5685	96.1135	1282.7	32.7783	96.0143
JBTB-38	−14.2	−106.6	7	3706	32.4106	96.4158	338	32.5389	96.3679
JBTB-39	−14.4	−103.2	12	3678	32.3663	96.4192	16664.6	33.0302	95.1273
JBTB-42	−16.9	−117.1	17.9	4115	31.9948	96.4148	4.5	31.9995	96.4217
JBTB-43	−15.7	−114.8	10.7	3628	31.7535	96.3343	12017.9	32.2842	95.2729
JBTB-46	−15.3	−112.9	9.9	3175	31.0201	97.2953	54390.1	32.4061	95.9964
JBTB-47	−16.8	−129.3	5	3175	31.0201	97.2953	343.9	31.1216	97.3573
JBTB-50	−18.3	−137.5	8.6	4323	30.5032	97.1473	269.5	30.462	97.0109
JBTB-51	−17.3	−130.2	8.5	4241	30.4406	97.1822	2710.3	30.6828	96.8751
JBTB-53	−17.5	−131.3	8.6	4252	30.1335	97.2749	2.1	30.1366	97.2695
JBTB-54	−17.7	−129.1	12.3	2885	30.0685	97.1593	3085.6	29.8822	96.8869
JBTB-55	−16.9	−124	11.3	3773	29.9597	96.6613	1110.2	29.7912	96.7149
JBTB-56	−16.8	−121.3	13	4111	29.7766	96.7081	297.8	29.7952	96.5816
JBTB-58	−15.9	−116.4	11.1	4248	29.5761	96.7548	231.3	29.6264	96.7003
JBTB-59	−15.5	−110.3	13.3	3224	29.6305	96.2731	1053.9	29.593	96.4194
JBTB-60	−16	−113.8	14.5	3224	29.6305	96.2731	314.4	29.7972	96.3048
JBTB-62	−14.1	−97.5	15.1	2687	29.9154	95.6284	4209.4	30.2874	95.5141
JBTB-63	−14.5	−104.9	10.9	2631	29.9352	94.801	739	29.7491	94.7076
				Snow					
JBTB-05	−12.19	−67	30.7	3806	35.8316	99.9184			
JBTB-11	−11.9	−56	38.9	4234	35.0131	98.0687			
JBTB-17	−8.74	−30	40	4216	34.6709	98.0459			
JBTB-19	−10.72	−52	33.5	4744	34.1132	97.647			
JBTB-21	−16.71	−108	25.9	4514	33.9708	97.3515			
JBTB-24	−17.41	−106	32.8	4577	33.14	97.4978			
JBTB-33	−13.53	−74	34.4	4498	32.8878	96.6926			
JBTB-41	−12.34	−65	33.7	4500	31.941	96.4786			
JBTB-45	−19.93	−135	24.9	4601	31.0783	96.9479			
JBTB-49	−19.42	−144	11.6	4350	30.5522	97.1056			

[a]The centroid is defined as the geographic center of a catchment upstream from a stream or river sample site. The centroid is the coordinate used in Figure 3 for data from this study.

2008]. Climate modeling suggests that a marine regression would lead to a stronger Asian monsoon and cooling of the continental interior [*Ramstein et al.*, 1997; *Zhang et al.*, 2007]. Pollen from the Qaidam Basin also suggest that a relatively dry period persisted from Eocene to Oligocene time, which *Wang et al.* [1999] attribute to meridional plate movement.

3. Methods

3.1. Modern Stream Water

[14] Water samples were collected in August of 2008 across the Tibetan Plateau from north to south (Figure 1 and Table 1). There were no significant precipitation events during our week of sampling, so surface waters are assumed to reflect summertime-integrated rainfall and groundwater composition. Surface water was collected from a wide variety of catchments including both small tributaries and large rivers. All samples were stored in plastic vials sealed with Teflon tape and refrigerated until analysis. Snow samples were allowed to melt in sealed vials. Oxygen isotopic analyses were conducted at the University of Rochester SIREAL laboratory. For oxygen analyses, ~0.5 mL of each water sample was loaded into a 12 mL Exetainer™ and flushed with a mixture of 0.3% CO_2 and UHP helium. Tubes were allowed to equilibrate for at least 18 h at ambient room

temperature prior to analysis. Headspace CO_2 gas was then drawn into a Thermo Delta plus XP mass spectrometer in continuous-flow mode via a Thermo Gas Bench peripheral and a GC-PAL autosampler for analysis. The $\delta^{18}O$ results are normalized using internal laboratory standards calibrated to Vienna Standard Mean Ocean Water (VSMOW) and Standard Light Antarctic Precipitation (SLAP) with 2σ uncertainties of 0.20‰. Hydrogen D/H ratios were analyzed at the University of Arizona using a dual-inlet mass spectrometer (Delta-S, Thermo Finnegan, Bremen, Germany) equipped with an automated chromium reduction device (H-Device, Thermo Finnegan) for the generation of hydrogen gas using metallic chromium at 750°C. Standardization was based on internal standards referenced to VSMOW and VSLAP. Precision is better than ±1‰ for δ^2H.

3.2. HYSPLIT Modeling

[15] We have used the HYbrid Single-Particle Lagrangian Integrated Trajectory Model (HYSPLIT) together with reanalysis model output from the Global Data Assimilation System (GDAS) data set [*Draxler and Hess*, 1998; *National Oceanic and Atmospheric Administration*, 2010; Draxler and Rolph, Web site, 2010] run at T170 horizontal resolution (~75 km) to compile an inventory of the origin of precipitation-producing air masses for six locations along a roughly south-north transect coinciding with sample locations, and for three sites along a parallel transect across the central plateau. The HYSPLIT algorithm and the GDAS data set are well documented in the above references.

[16] For each of the six locations, 10-day (240-h) back trajectories were computed every 12 h for the years 2004–2009. In this paper we show precipitation-producing 72-h back trajectories that were initialized 1km above ground level during the months of June, July, and August. This filtering is done to (1) focus on vapor-rich air parcels, as most water vapor in the atmosphere is within 0–2 km above ground level [*Wallace and Hobbs*, 2006; section 2.2], (2) limit results to air masses that have not undergone substantial recycling, as the average lifetime of water vapor in the atmosphere is several days to a week [*Wallace and Hobbs*, 2006, section 9.3], and (3) focus on months that receive the most precipitation (auxiliary material Figure S1). Results are consistent with other reasonable choices for initialization altitude (100 m, 500 m, 1 km, and 2 km) and duration of back trajectory (24 to 240 h). Trajectories are considered precipitation-producing if there is precipitation from the air parcel within twelve hours of reaching the location of interest.

[17] Others have used HYSPLIT together with water isotope measurements to diagnose the origin and isotopic signature of precipitation-producing air masses with considerable success [e.g., *Buda and DeWalle*, 2009; *Sjostrom and Welker*, 2009; *Breitenbach et al.*, 2010]. More broadly, HYSPLIT is used to determine the origin and chemistry of precipitation-producing air masses worldwide [e.g., *Jorba et al.*, 2004; *Butler et al.*, 2001; *Zunckel et al.*, 2003]. Nevertheless, there are two primary limitations to this analysis. First, it is based on winds derived from the GDAS reanalysis and is therefore subject to any errors in the GDAS data set. Reanalysis models utilize both observations and a global-scale numerical weather model to give the community's best estimate of the global atmosphere. However, they are subject to errors especially in regions of rugged terrain and where observations are limited [*Kalnay et al.*, 1996]. Second, HYSPLIT is an air-parcel, not a water vapor, back trajectory algorithm. The addition and removal of water vapor from the air mass is not included in this analysis so we cannot infer the relative importance of local moisture sources to precipitation. Limitations are ameliorated because we calculate thousands of trajectories, focusing on bulk and large-scale characteristics rather than any single trajectory.

4. Results

4.1. Stable Isotopes of Surface Water

[18] The southernmost samples in this transect were collected in the high Himalaya along the upper reaches of the Brahmaputra drainage (Figure 1). The $\delta^{18}O$ values are significantly more negative (average = −15.7‰) compared to lower elevation sites in the Himalayan foreland (average = −6.7‰ from *Hren et al.* [2009]) (Figure 3). Our results from the northeastern margin of the plateau (samples from latitude >35°N) also show an inverse relationship between $\delta^{18}O$ and elevation of −2.3‰/km with $R^2 = 0.83$ (Table 1), which is a slightly lower lapse rate compared to the central Himalaya (−2.9‰/km from *Garzione et al.* [2000a]).

[19] Samples from high elevations in the Himalaya show relatively high *d excess* values (average = 12.3‰) compared to low elevation (<1000 m) stream water in the Himalayan foreland (average = 7.3‰ from *Garzione et al.* [2000a]) and precipitation in New Delhi (long-term weighted average = 8.9‰ from IAEA/WMO (Web site, 2010)) (Figure 6). These low elevation data contrast anomalously high *d excess* values from low elevation tributaries of the Brahamaputra sampled in early February (average = ~14.5‰ from *Hren et al.* [2009]), likely reflecting the unique isotopic signature of winter precipitation in the Himalaya [*Tian et al.*, 2005]. These results suggest that there is an inverse relationship between $\delta^{18}O$ and *d excess* up the windward side of the Himalaya, observed along its length from the Indus to Brahmaputra Rivers [*Garzione et al.*, 2000a; *Karim and Veizer*, 2002].

[20] From the high Himalaya into southern Tibet, *d excess* of surface water decreases significantly from an average of 12.3‰ to ~8.5‰, without an associated change in $\delta^{18}O$ (Table 1). This shift occurs across the Salween River which is the threshold delineating catchments that draw from Himalayan precipitation with high *d excess* and those that source more arid regions on the plateau with lower *d excess*. A visible change in climate is also observed along the road (highway 318) as one travels through the Salween drainage into the Brahmaputra drainage.

[21] Across the Tibetan Plateau, there is no apparent relationship between latitude and *d excess* when all stream and river water samples are considered. However, when the data set is filtered to only include large rivers (catchments >1000 km^2), we observe a systematic increase in *d excess* from ~8.5‰ in the southern plateau to ~14‰ in the north (Figure 4b). Smaller streams and tributaries show pronounced variation in *d excess* over small distances, likely because they are affected by local variations in climate and topography [e.g., *Barros et al.*, 2006; *Froehlich et al.*, 2008] that larger catchments may effectively average out. River water *d excess* values from *Tian et al.* [2001] on the central

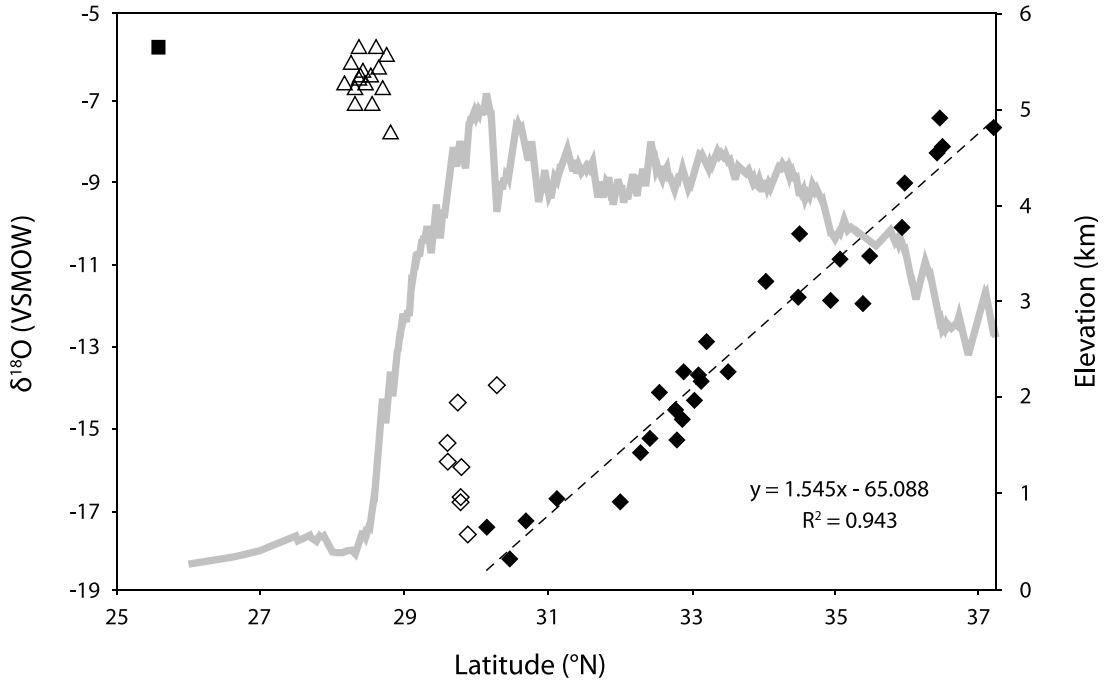

Figure 3. A compilation of meteoric water $\delta^{18}O$ values from sites along a transect from south to north (Figure 1). Open and closed diamonds are surface water samples from this study. Open diamonds represent water samples collected on the windward side of the Himalaya and solid diamonds were collected across the Tibetan Plateau. The gray curve is the average elevation over a 200 km wide swath following the transect. The linear regression is calculated from samples on the Tibetan Plateau (closed diamonds). Open triangles are low elevation (<700 m) surface water samples from the Himalayan foreland reported by *Hren et al.* [2009]. The solid square is the long-term weighted annual $\delta^{18}O$ of precipitation at Shilong, India (IAEA/WMO Web site, 2010). The geographic center of catchments upstream from stream or river sample sites (centroid) is used for data from this study (all diamonds).

plateau agree surprisingly well with our results, with the exception of one uniquely low value (∼7‰) from the Amdo River at ∼32.3° latitude, which is excluded from our regression (Figure 4b). A progressive increase in *d excess* from south to north is consistent among data sets across the entire plateau [*Tian et al.*, 2001; *Yu et al.*, 2007].

[22] The $\delta^{18}O$ values of surface water also increase by ∼1.5‰ per degree latitude northward across the plateau (R^2 = 0.94) (Figure 3). This is consistent with parallel transects further west in the central plateau which also show a composite lapse rate of ∼1.5‰ per degree latitude [*Quade et al.*, 2011]. Snow samples track surface water $\delta^{18}O$ closely on the plateau, as the average difference between snow samples and their nearest surface water samples is <1‰ (Table 1). However, *d excess* values from snow are consistently much higher (average ∼20‰) than surface water sampled nearby (Table 1).

4.2. Rayleigh Distillation Model for the Tibetan Plateau

[23] Rayleigh distillation of an air mass under equilibrium conditions without local evaporation or advection of additional vapor from outside the system causes a progressive decrease in the $\delta^{18}O$ value of precipitation [*Rozanski et al.*, 1993; *Gat*, 1996]. Subcloud evaporation of raindrops can significantly attenuate this decrease in $\delta^{18}O$. However, evaporation in the air column causes *d excess* of precipitation to decrease which is not consistent with observations on the Tibetan Plateau [*Gat and Airey*, 2006; *Froehlich et al.*, 2008]. Here, we test whether recycling of relatively enriched surface waters can account for the observed increase in both $\delta^{18}O$ and *d excess* with latitude across the Tibetan Plateau (Figures 3 and 4b) with a model of Rayleigh distillation modified by surface water evaporation.

[24] We model the isotopic evolution of a vapor mass that experiences six precipitation events where 20% of available vapor condenses as precipitation at each step [*Fankhauser*, 1988; *Schoenberg Ferrier et al.*, 1996]. Refer to the Appendices A and B and auxiliary material Table S1 for a detailed explanation of model input parameters and calculations. We note that the number of precipitation events has no significant effect on the model output, and results would be similar if a larger number of steps were used. Six precipitation events were chosen to reflect the six sites for which we carried out back trajectory analysis using HYSLIT. We use the Rayleigh distillation equation (equation (A1) in Appendix A) to calculate the isotopic composition of reservoir and product phases after precipitation and/or evaporation. We assign the vapor mass an initial $\delta^{18}O$ value of −27.7‰ and $\delta^{2}H$ value of −209‰ which produces a first rain with $\delta^{18}O$ of −18.1‰ and *d excess* of ∼7.6‰, matching observation on the southern Tibetan Plateau (Figures 3 and Figure 4b). Temperatures of condensation across the plateau are based on the dew point, which is calculated from surface temperature and relative

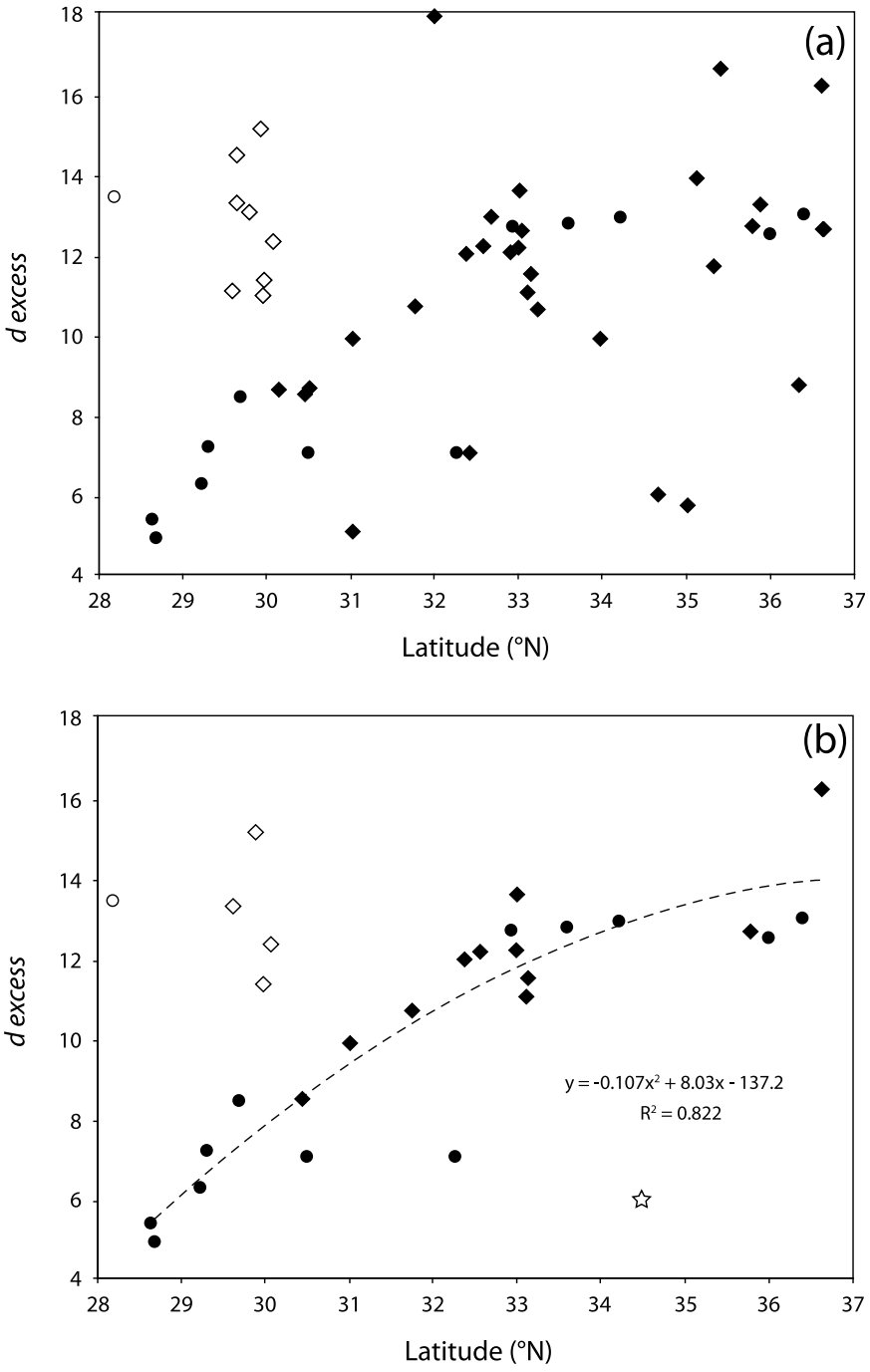

Figure 4. Deuterium excess (*d excess*) values of rivers and tributaries in the Himalaya and on the Tibetan Plateau, plotted against absolute latitude of the sample site. (a) Data from rivers of all sizes and (b) Deuterium excess (*d excess*) values of only large rivers (catchments >1000 km^2). Data from this study (closed diamonds) are from a south-north transect on the eastern Tibetan Plateau. Closed circles show data from *Tian et al.* [2001] along a roughly parallel transect further west on the central plateau. Open diamonds represent river water samples from the high eastern Himalaya which is at the same latitude as samples from the central Tibetan Plateau due to the arcuate shape of the Himalayan front. Open circle is a sample from the high central Himalaya [*Tian et al.*, 2001]. The regression (Figure 4b) is made through all samples from the Tibetan Plateau (closed diamonds and circles). The river sample represented by an open star was not included in the regression as its uniquely low value is not likely to represent regional trends. The geographic center of catchments (centroid) was not used because this information is unavailable for the *Tian et al.* [2001] data set. See Figure 1 for the location of each transect.

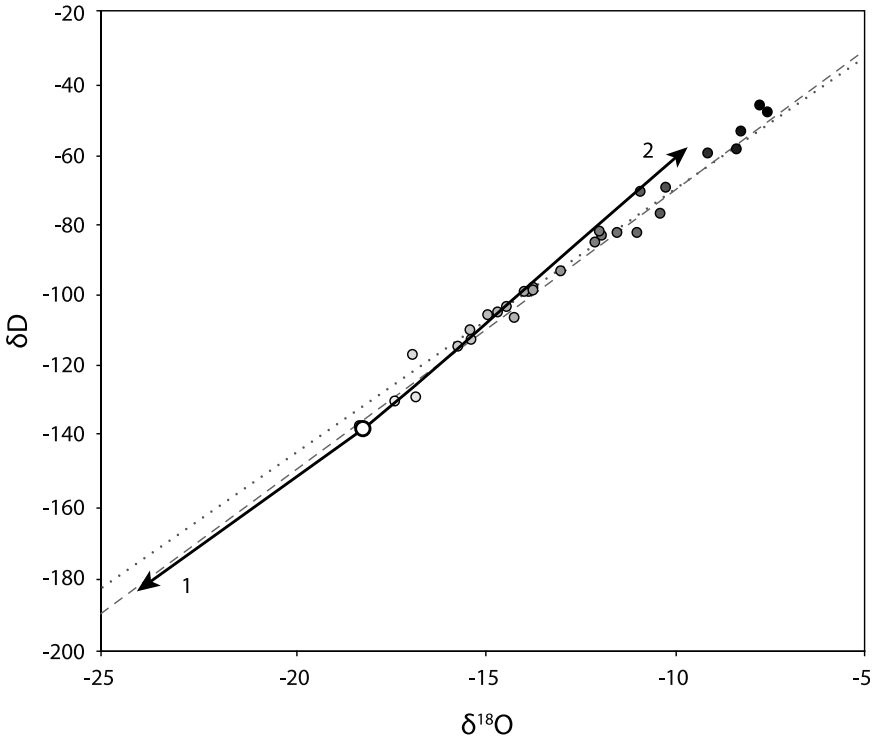

Figure 5. The theoretical evolution of precipitation $\delta^{18}O$ and $\delta^{2}H$ across the Tibetan Plateau through Rayleigh distillation of an air mass modified by evaporation of surface waters. Small circles show the isotopic composition of surface water from large rivers (this study and *Tian et al.* [2001]) collected across the plateau from south (white fill) to north (black fill). Dashed gray line is the Global Meteoric Water Line (GMWL) and dotted line is the local meteoric water line (LMWL) defined by the equation y = 7.67x + 6.7. The isotopic composition of the first precipitation (large open circle) is assigned a value to be consistent with observation on the southern plateau. Curve 1 represents the evolution of precipitation assuming Rayleigh distillation under equilibrium conditions without evaporation or kinetic fractionation. Curve 2 represents the modeled evolution of precipitation assuming Rayleigh distillation modified by recycling of surface water. In order to evolve both $\delta^{18}O$ and *d excess* to more positive values as shown in curve 2, surface water $\delta^{18}O$ and the recycling ratio must both increase downwind while relative humidity decreases. A detailed discussion of model parameters and calculations can be found in Appendix A and auxiliary material Table S1.

humidity using NCEP/NCAR reanalysis data. The temperatures of evaporation from surface water are estimated from soil water [*Yamada and Uyeda*, 2006; *Yang et al.*, 2007b] and surface air temperatures [*Yu et al.*, 2006; *National Oceanic and Atmospheric Administration*, 2010] during summer months (JJA). The change in relative humidity across the plateau (Figure 2) is used to calculate kinetic fractionation (equation (A5) in Appendix A) associated with evaporation of surface water [e.g., *Gonfiantini*, 1986]. Surface water may include lakes, streams, and soil water, all of which recycle moisture back into the atmosphere. Lakes on the Tibetan Plateau can have $\delta^{18}O$ values that are ~10–15‰ more positive than local precipitation while soil water has been shown in Hawaii to be ~5‰ more positive than stream water [*Hsieh et al.*, 1998]. In Xinjiang, soil water evaporation contributes an order of magnitude less moisture to the atmosphere compared with lake and stream water [*Pang et al.*, 2011]. Therefore, we use published lake water isotopic values for the recycled fraction on the plateau, recognizing that stream and soil water evaporation may mitigate the effects of surface water recycling. The surface water reservoir is set to be 2 orders of magnitude larger than the vapor mass as the volume of surface water on the Tibetan Plateau far exceeds the volume of water vapor in the atmosphere. Increases in the relative size of the surface water reservoir beyond 2 orders of magnitude have no significant effect on isotopic results. The evaporative flux from surface waters is determined by the recycling ratio for each step, defined as the ratio of locally evaporated (continental) to advected vapor (oceanic) in the air mass [*Brubaker et al.*, 1993; *Trenberth*, 1999]. Model results show that Rayleigh distillation modified by surface water recycling causes both $\delta^{18}O$ and *d excess* values of precipitation to increase (curve 2 in Figure 5), consistent with observation of surface water $\delta^{18}O$ and *d excess* across the Tibetan Plateau. The environmental conditions necessary to model this effect are: (1) Surface water $\delta^{18}O$ must increase downwind, (2) The recycled fraction of moisture in precipitation (the recycling ratio) must increase downwind, and (3) Relative humidity at the surface must decrease downwind.

4.3. Model of Rayleigh Distillation in the Himalaya

[25] In the case of the windward side of the Himalaya, it has been shown that there is an inverse relationship between

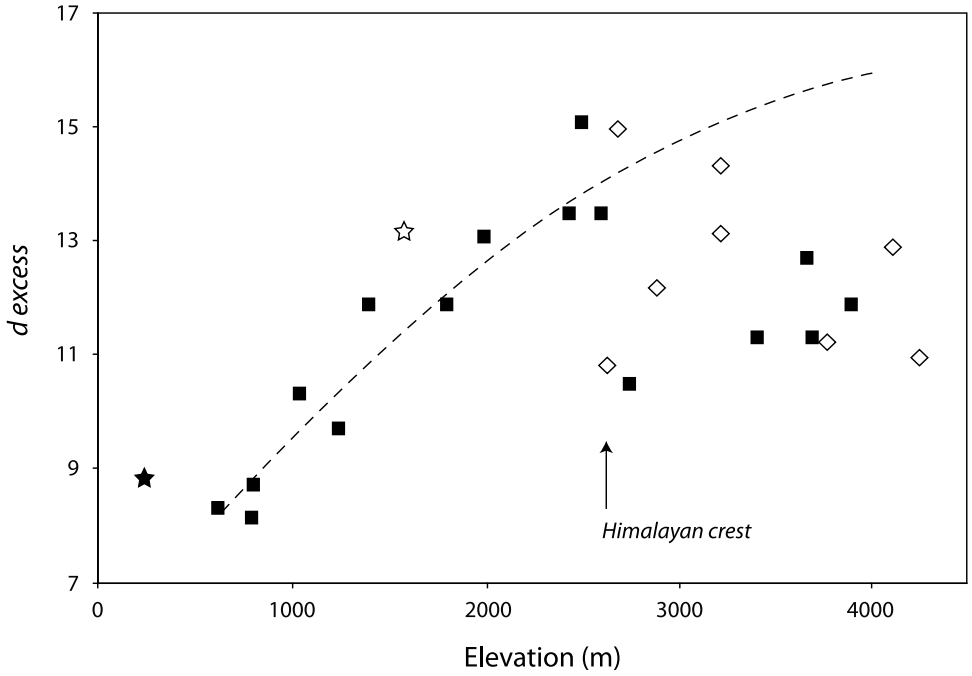

Figure 6. Deuterium excess (*d excess*) values of river water and stream water from the Himalaya plotted against sample site elevation. Data from this study (open diamonds) are from the upper reaches of the Brahmaputra drainage (Figure 1). Solid squares are tributaries of the Kali Gandhaki river in the central Himalaya published by *Garzione et al.* [2000a]. Filled star and open star are the annual weighted average *d excess* of precipitation at New Delhi and Shilong, India respectively (IAEA/WMO Web site, 2010). Dashed line represents *d excess* of precipitation based on Rayleigh distillation where condensation occurs at progressively colder temperatures (27.5°C to −7°C) up the windward flank of the Himalaya (refer to Appendix B and auxiliary material Table S1 for model parameters and calculations).

δ^{18}O values of meteoric water and elevation [*Garzione et al.*, 2000a], consistent with Rayleigh distillation of vapor as it is orographically lifted and adiabatically cooled by the range front. Surface water data from this study and others [*Garzione et al.*, 2000a; *Karim and Veizer*, 2002] suggest that *d excess* co-varies with elevation along the same transects. We model the isotopic composition of precipitation distilled at progressively colder temperatures (27.5°C to −7°C) from the Himalayan foreland to the high Himalaya using initial δ^{18}O and *d excess* values of −8.4‰ and ∼8‰ respectively, based on low elevation surface water reported by *Garzione et al.* [2000a]. Temperatures of condensation are approximated as the surface dew point temperature (equation (A2) in Appendix A) using the mean summer (JJA) surface air temperature (*T*) at New Delhi (the Himalayan foreland) and at ∼6000 m near Mt. Qomolangma (Everest) which are ∼31.5°C and ∼−3°C respectively [*Xie et al.*, 2006; IAEA/WMO Web site, 2010], and the relative humidity (*RH*) at both sites which is ∼80% (Figure 3). Results show that Rayleigh distillation, assuming equilibrium fractionation at progressively colder temperatures of condensation, causes *d excess* to increase in precipitation, consistent with observations in the Himalaya (Figure 6). Other possible reasons for the observed increase in *d excess* with elevation are discussed in section 5.1.1.

4.4. HYSPLIT Modeling of Air Mass Contribution

[26] The climatology of precipitation-producing back trajectories is shown for six locations in Figure 7a. For each panel in Figure 7a, a large red square corresponds to the location of interest for all back trajectories. The small dots correspond to the location of each air parcel 72 h before reaching the location of interest, and gray shading indicates the density of these dots. Trajectories were calculated twice a day for summer months (JJA), from 2005 to 2009. Therefore, 920 total trajectories were computed at each location, and only the precipitation-producing trajectories are shown.

[27] Along the south-north transect, there is a general preference for air to emanate from one of three directions, which we refer to as the southerly (coming from the south), northwesterly, and easterly source regions. It is notable that none of the back trajectories extend to an ocean, which is a strong indication that continental recycling of moisture is significant. On the southern and central plateau (the 3 southern-most sites), almost all air masses arrive from the southerly source region. On the northeast margin of the plateau, however, the southerly source region plays a much smaller role; in these regions, easterly and northwesterly sources dominate. In the lower elevation region beyond the northeastern margin of the Tibetan Plateau (the 2 northern-most sites), air masses are derived exclusively from easterly and northwesterly sources. We also calculate back trajectories along a meridional transect in the central Tibetan Plateau shown in Figure 7b. These back trajectories are analagous to those along the eastern transect in that they show a predominantly southerly source across at least two thirds of the width of the

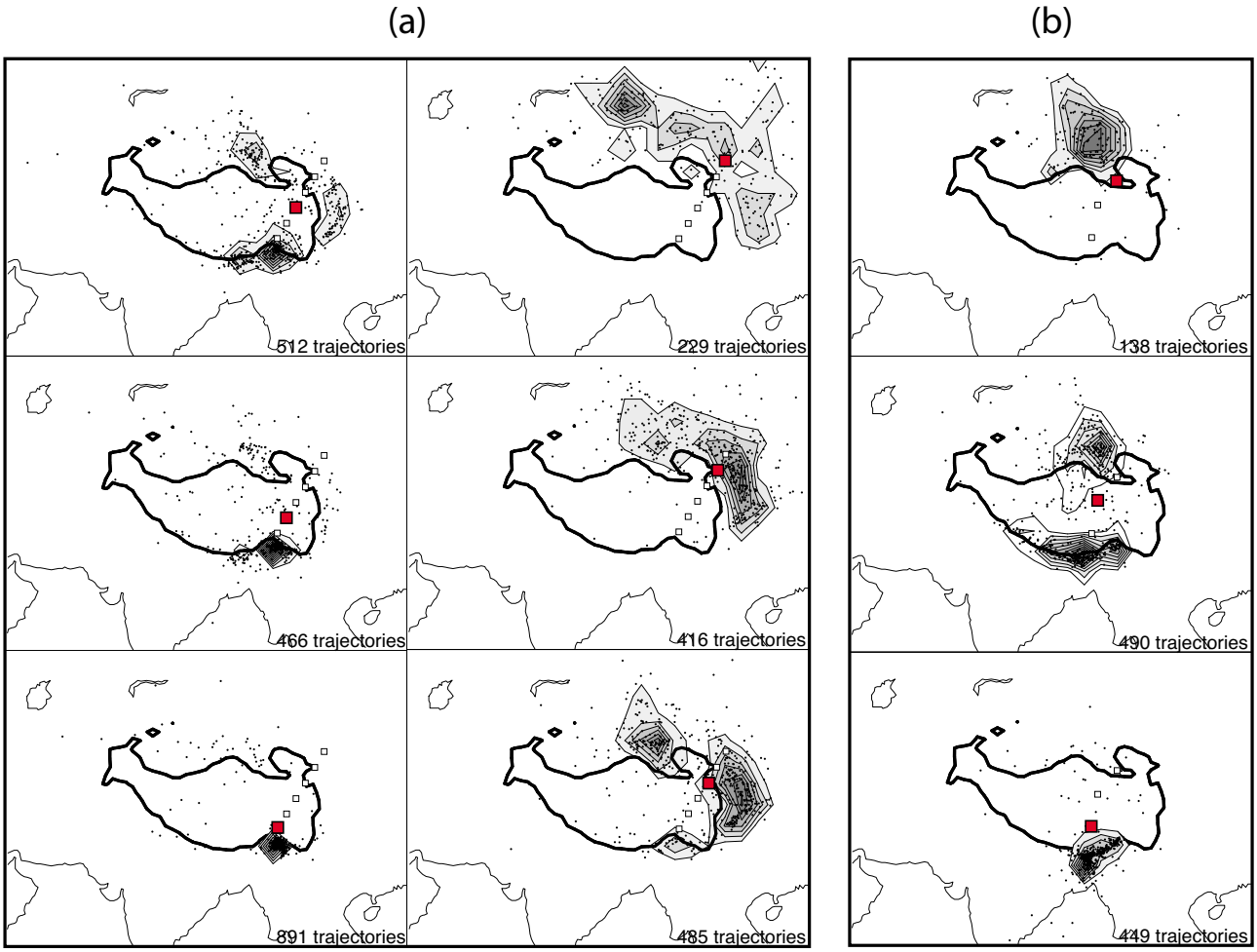

Figure 7. (a) HYSPLIT back trajectories showing the location of summertime (JJA) precipitation-producing air parcels (black dots) 72 h prior to their arrival at one of six sites (red squares). Back trajectory sites follow our south-north sampling transect on the eastern Tibetan Plateau. 2-D histograms represent air parcel origin density. Dark black outline is the 3500 m elevation contour. (b) HYSPLIT back trajectories with the same boundary conditions shown in Figure 7a. These 3 back trajectory sites follow a roughly parallel transect on the central Tibetan Plateau similar to that described by *Tian et al.* [2001]. The 2-D histograms represent air parcel origin density. Again, the dark black outline is the 3500 m elevation contour.

plateau, with one notable exception: the central Tibetan Plateau does not show an easterly source region.

[28] The back trajectories indicate flow patterns that are reasonable for atmospheric circulations in this region. For example, there is a systematic decrease in the number of precipitation-producing trajectories from the south to the north, consistent with observations of precipitation amount across the plateau (IAEA/WMO Web site, 2010). In addition, the trajectories have preferred source regions, but these source regions are quite diffuse indicating that atmospheric flow patterns are variable. One surprising result is that the most southerly trajectories in the eastern Tibetan Plateau transect emanate from a small region in the Brahmaputra delta (Figure 7a), whereas in the central transect, these southerly trajectories are more widely distributed. While this strong localization on the eastern Tibetan Plateau is certainly possible, this may be a model artifact; small errors in modeled winds near steep topography could give rise to this phenomenon. Regardless, there is no doubt that the southerly trajectories emanate from south of the Himalaya. Though it seems likely that northwesterly back trajectories are ultimately derived from midlatitude westerlies with origins in the Atlantic and/or Mediterranean, it is also possible that they are related to Pacific-derived vapor that makes its way around the northeast margin of the Tibetan Plateau. Distinguishing between these possibilities is beyond the scope of this study.

5. Discussion

5.1. Controls on $\delta^{18}O$ and $\delta^{2}H$ of Modern Meteoric Water

[29] An understanding of modern isotopic evolution in meteoric water across the Himalaya and Tibetan Plateau is necessary for interpretation of past changes in elevation and climate from isotopes preserved in the geologic record. Our isotopic results from surface waters across the eastern Himalaya and Tibetan Plateau show trends consistent with roughly parallel transects further west [*Garzione et al.*,

2000a; *Tian et al.*, 2001; *Karim and Veizer*, 2002; *Quade et al.*, 2007; *Yu et al.*, 2007]. However, HYSPLIT back trajectories along the eastern plateau transect (Figure 7a) show an easterly source region which is absent within the central plateau transect (Figure 7b). Consistent trends in $\delta^{18}O$ and *d excess* along N-S transects across the plateau, regardless of changes in source region, suggest that a local process, such as continental recycling, may overprint the original isotopic signature of source moisture.

5.1.1. The Margins of the Himalaya and Tibetan Plateau

[30] Results show an inverse relationship between $\delta^{18}O$ and elevation up the Brahmaputra drainage (Figure 3), consistent with Rayleigh distillation of vapor as it is orographically lifted and adiabatically cooled. This trend is now documented along the Himalayan front [*Garzione et al.*, 2000a; *Karim and Veizer*, 2002; *Hren et al.*, 2009], around the eastern syntaxis [*Hoke et al.*, 2008], and up the plateau's eastern margin [*Yu et al.*, 1984]. Tributaries (catchments <1000 km^2) on the northeast margin of the Tibetan Plateau (latitude >35°) show an isotopic lapse rate of −2.1‰/km with R^2 = 0.85 (Table 1). However, this isotopic lapse rate decreases to only −0.8‰/km (R^2 = 0.53) when corrected for changes in $\delta^{18}O$ with latitude (discussed in section 5.1.3).

[31] Considering that this region receives the majority of its precipitation during the summer months (JJA) (auxiliary material Figure S1) and that the Himalaya and eastern margin of the Tibetan Plateau are proximal to the Bay of Bengal and South China Sea, the majority of precipitation in these areas is likely ultimately derived from the Indian and east Asian monsoons. However, high *d excess* values throughout the high Himalaya (average = 12.3‰ from this study) relative to lower elevations in the Himalayan foreland (Figure 6) suggest that a significant amount of high elevation precipitation may be transported to the region during the winter and early spring by westerlies from a Mediterranean source [*Karim and Veizer*, 2002; *Tian et al.*, 2005; *Hren et al.*, 2009] as it is on the northwestern flank of the Tian Shan [*Numaguti*, 1999]. This is consistent with studies in the Himalaya and elsewhere that suggest unique sources of precipitation may be prevalent at different elevations along range fronts [*Holdsworth and Krouse*, 2002; *Barros et al.*, 2006].

[32] However, it is also possible that progressively lower temperatures of condensation at higher elevations in the Himalaya also cause *d excess* values to increase as predicted by Rayleigh distillation under equilibrium conditions (see dashed curve in Figure 6, Appendix B, and Table S1) [e.g., *Jouzel and Merlivat*, 1984]. The same relationship between elevation and *d excess* is observed in precipitation up the windward side of the Andes [*Gonfiantini et al.*, 2001] and in Antarctica [*Petit et al.*, 1991], indicating that a Mediterranean source for the high *d excess* of precipitation is not a unique explanation for these trends. Instead, low relative humidity over oceanic source regions during winter months may cause an increase in *d excess* of high elevation precipitation worldwide [*Jouzel et al.*, 1997]. Other local processes may also contribute to relatively high *d excess* values in the high Himalaya such as local moisture recycling, reduced subcloud evaporation, and/or increased contributions from orographic fog [*Liotta et al.*, 2006; *Scholl et al.*, 2007; *Froehlich et al.*, 2008; *Cui et al.*, 2009].

5.1.2. The Himalayan Rainshadow

[33] On the leeward side of the Himalaya, results show that *d excess* values of surface water shifts by −3.8‰ from an average of 12.3‰ in the high Himalaya to 8.5‰ immediately north (Table 1), consistent with a shift from high *d excess* snow on Qomolongma (Mt. Everest) (>10‰) to lower values in precipitation (4.1‰) just ∼50 km north in Tingri [*Kang et al.*, 2002]. Low *d excess* values for surface water are also observed along the upper Yarlung Tsangpo river (average = 4‰ from *Hren et al.* [2009]) located less than 200 km north of the Himalayan crest, and in river water south of the Tanggula Mountains on the central Tibetan Plateau (average = 6.6‰) (Figure 4b) compared to high elevations in the central Himalaya and northern plateau where *d excess* >10‰ [*Tian et al.*, 2001, 2005]. These studies attribute relatively low *d excess* values on the southern plateau to monsoon versus westerly derived precipitation, though *Kang et al.* [2002] suggest local weather conditions may also contribute.

[34] This drop in *d excess* values may be due to a change in climate from the windward side of the Himalaya into its rainshadow, where evaporation of raindrops falling through a lower humidity air column result in lower *d excess* values of precipitation [e.g., *Araguás-Araguás et al.*, 1998; *Gupta and Deshpande*, 2003; *Peng et al.*, 2009]. This effect is demonstrated on the central Tibetan Plateau where *d excess* of precipitation increases throughout the lifecycle of storms due to moistening of the ground surface and air column which reduces subcloud evaporation [*Kurita and Yamada*, 2008]. A similar negative shift to relatively low *d excess* in the rainshadow of the Andes is seen in precipitation from high in the eastern Cordillera (∼18‰ from *Gonfiantini et al.* [2001]) to La Paz, Bolivia (annual weighted mean = 12.6‰ from IAEA/WMO Web site, 2010), consistent with subcloud evaporation of raindrops over the relatively arid Altiplano.

5.1.3. The Tibetan Plateau

[35] Northward across the plateau, there is a positive trend in meteoric water $\delta^{18}O$ that is linear (∼1.5‰ per degree latitude) and robust (R^2 = 0.94) (Figure 3). As we previously noted, this is remarkably consistent with roughly parallel transects further west for both precipitation and surface water [*Tian et al.*, 2001; *Quade et al.*, 2007; *Yu et al.*, 2007]. Considering the Tibetan Plateau maintains an elevation of ∼5 km, this trend cannot be attributed to a decrease in elevation. Instead, the steady and consistent increase in $\delta^{18}O$ may reflect an increase in the contribution of westerly and/or continental-derived moisture northward [*Tian et al.*, 2001; *Quade et al.*, 2007; *Yu et al.*, 2008].

[36] Our modeling and HYSPLIT results suggest that monsoon-derived precipitation, originating over the Indian and/or South Pacific Ocean, dominates the hydrological budget of the southern, eastern, and possibly central Tibetan Plateau. This is consistent with the observation that precipitation on the Tibetan Plateau and its margins falls predominantly during summer months (auxiliary material Figure S1), which generally coincides with Indian and east Asian monsoon rainfall.

[37] HYSPLIT back trajectories are consistent with the interpretation that the original oceanic source of moisture changes from the southern to northern Tibetan Plateau [*Tian et al.*, 2001; *Quade et al.*, 2007; *Yu et al.*, 2008]. However, HYSPLIT results also suggest that the relative contribution of

air masses derived from unique source regions varies across the plateau from east to west (Figures 7a and 7b) despite consistent trends in both $\delta^{18}O$ and *d excess* along parallel N-S transects (Figures 3 and 4b) [*Tian et al.*, 2001; *Yu et al.*, 2007]. Accordingly, it is possible that an increasing fraction of recycled surface water in precipitation from south to north across the plateau is causing the observed positive trend in $\delta^{18}O$, regardless of changes in original oceanic source.

5.1.4. Air Mass Mixing Models for the Northern Tibetan Plateau

[38] Air mass mixing models, where multiple vapor sources with distinct isotopic signatures mix in different proportions across the plateau, have been used to explain the trends in both *d excess* and $\delta^{18}O$ for the Himalaya and Tibetan Plateau [*Karim and Veizer*, 2002; *Yang et al.*, 2006]. However, Mediterranean (~20‰) [*Gat and Carmi*, 1970], Indian and Pacific Ocean (~10‰), and Arctic (<10‰) [*Dansgaard*, 1964] end-members should be used with caution because it has been demonstrated that *d excess* is substantially affected by processes during transport in this region [*Numaguti*, 1999; *Gupta and Deshpande*, 2003; *Yamada and Uyeda*, 2006; *Kurita and Yamada*, 2008]. That said, sites along the western edge of the Pamir plateau and Tian Shan receive precipitation primarily during winter and/or spring months (auxiliary material Figure S1), consistent with seasonal precipitation in the Mediterranean basin (IAEA/WMO Web site, 2010). Urumqi (Wulumuqi), China, is a Global Isotopes in Precipitation (GNIP) site located in the Tian Shan that intercepts westerlies [*Aizen et al.*, 1997; *Tian et al.*, 2007; *Pang et al.*, 2011] en route to the Tibetan Plateau. It has an extended rainy season with precipitation falling primarily during the spring and summer (auxiliary material Figure S1). Urumqi's amount weighted average *d excess* for spring (MAM) is ~11.7‰ and summer (JJA) is ~8.5‰, both consistent with Arctic or monsoon derived moisture (IAEA/WMO Web site, 2010). Winter precipitation (DJF) *d excess* is much higher at ~21‰ (IAEA/WMO Web site, 2010), more typical of Mediterranean (westerly) sourced precipitation. This is consistent with HYSPLIT back trajectories that show the northwesterly source region is more prevalent in the winter months compared to summer months (not shown). Though the winter is relatively dry in Urumqi and on the Tibetan Plateau, it is possible that the relative contribution of winter-time precipitation via westerlies increases northward across the Tibetan Plateau. However, to fully account for the increase in *d excess* observed in surface water northward across the plateau that reaches a maximum of ~14 to 16‰ (Figure 4), winter precipitation would have to provide ~50% of the annual total. This assumes equal mixing between winter (~20‰) and summer (~10‰) end-members and is inconsistent with records around the plateau margins that show the majority of precipitation falls during summer months, though precipitation during winter months may be significant at high elevations on the northern plateau, as is observed in the high Himalaya (auxiliary material Figure S1) [*Tian et al.*, 2005].

5.2. Implications for Paleoclimate and Paleoelevation Reconstructions

[39] The modern $\delta^{18}O$ versus elevation lapse rate up the Himalaya (−2.9‰/km from *Garzione et al.* [2000a]), caused by Rayleigh distillation of an air mass under near equilibrium conditions, is likely to apply to paleowaters in the proto-Himalaya if precipitation was derived from a nearby ocean under similar temperature and relative humidity conditions [*Rowley and Garzione*, 2007]. Given the low latitude setting, this appears to be the case at least since collision with Eurasia ~45–55 Ma [*Rowley*, 1996; *Searle et al.*, 1997; *Zhu et al.*, 2005] as either the Neo-Tethys or Indian Ocean has been directly south of Eurasia throughout the Cenozoic [*Scotese et al.*, 1988; *Ali and Aitchison*, 2008]. Though it has varied in intensity, the monsoon was likely active throughout the entire Cenozoic as the persistence of a high (~4000 m) proto-Himalaya [*Molnar et al.*, 2010] alone may be enough to drive Indian monsoon circulation [*Boos and Kuang*, 2010].

[40] The isotopic composition of surface water on the northeast margin of the Tibetan Plateau is on average ~6‰ more positive compared to similar elevations in the Himalaya (Figure 3 and Table 1). Our results suggest that this may be due to a large continental recycled fraction in precipitation on the northern plateau. This northward increase would be reduced by the existence of an inland sea in communication with the ocean, such as the Paratethys seaway, as has been documented in the Tarim Basin during late Cretaceous, Paleogene, and as recently as middle Miocene time [*Wang et al.*, 1992; *Ritts et al.*, 2008; *Bosboom et al.*, 2010]. The effect an inland sea would have on $\delta^{18}O$ values might not be substantial considering that sites in the Mediterranean Basin (an analog that might resemble marine conditions in the Tarim Basin) show precipitation $\delta^{18}O$ values near −8‰ at ~1000 m elevation [*Gat et al.*, 1996; *Liotta et al.*, 2006], similar to modern surface water on the northeast margin of the Tibetan Plateau (Figure 3).

[41] When the latitudinal change in the $\delta^{18}O$ values of modern meteoric water is incorporated into paleoelevation estimates for the central and northern plateau, the effect is significant. We take a similar approach to that of *Quade et al.* [2011] to quantify this effect for the northern Tibetan Plateau. Fenghuoshan carbonates from the Hoh Xil Basin, currently at ~5000 m on the northern Tibetan Plateau, suggest paleowater $\delta^{18}O$ was an average of −9.7‰ ± 2.1 during Eocene-Oligocene time [*Cyr et al.*, 2005]. This should be considered a minimum value as these rocks have undergone significant thermal alternation [*Polissar et al.*, 2009] which might cause a negative shift in $\delta^{18}O$ [e.g., *Garzione et al.*, 2004]. A general increase in $\delta^{18}O$ of ocean water since the Eocene [*Zachos et al.*, 2001] likely caused a wholesale increase in the isotopic composition of global precipitation. This consideration decreases paleoelevation calculations, increasing estimates of elevation gain. Correcting for the isotopic composition of ocean water at low latitude due to less ice volume in the late Eocene (−2‰ from *Zachos et al.* [1994, 2001]) gives a revised paleoelevation of ~800 m. Assuming precipitation was primarily sourced from the south (Neo-Tethys) with an increasing recycled fraction inland as is observed today, a third correction can be applied using the modern latitude-$\delta^{18}O$ relationship (~5° latitude causes $\delta^{18}O$ to increase by ~7.7‰ from Figure 3) which increases the paleoelevation estimate substantially to ~3500 m. This is ~1500 m lower than the Hoh Xil Basin today, but much higher than the paleoelevation estimate by *Cyr et al.* [2005] of ~2040 m. The latter is based on a Rayleigh distillation model that incorporates the $\delta^{18}O$ value and

temperature of contemporaneous vapor at its oceanic source [e.g., *Rowley et al.*, 2001].

[42] Paleowater $\delta^{18}O$ derived from Miocene plant wax in the Wudaoliang Formation in the same basin (Hoh Xil) averages $-13.9‰ \pm 0.3$ [*Polissar et al.*, 2009]. Accounting for differences in Miocene ocean $\delta^{18}O$ due to lower global ice volume ($\sim -1.5‰$ from *Zachos et al.* [2001]) and applying the same correction for the latitudinal change ($\sim 7.7‰$ from Figure 3) gives a paleoelevation estimate similar to modern of ~5100 m, considerably higher than the ~3500–4000 m calculated by *Polissar et al.* [2009]. Both estimates suggest that the northern Tibetan Plateau rose by ~1500 m from late Eocene to Miocene time. The assumption that continental recycling has had as profound an effect on isotopes on the northern Tibetan Plateau in the past as it does today results in higher paleoelevation estimates throughout the history of the plateau.

6. Conclusions

[43] We constrain mechanisms responsible for the isotopic evolution of meteoric water across the Himalaya and Tibetan Plateau by considering new surface water data in the context of a simple Rayleigh distillation model and HYSPLIT air mass back trajectories. Surface water $\delta^{18}O$ and $\delta^{2}H$ results from a roughly south-north transect on the eastern margin of the Tibetan Plateau are consistent with trends observed further west and along the plateau margins (Figure 1). Specifically, results corroborate consistent $\delta^{18}O$ lapse rates along the eastern and southern margins of the Tibetan Plateau and Himalaya respectively that are also close to the global average [*Garzione et al.*, 2000a; *Poage and Chamberlain*, 2001]. Results show a linear and robust relationship between $\delta^{18}O$ and latitude (Figure 3), as has been documented on the central Tibetan Plateau [*Tian et al.*, 2001; *Quade et al.*, 2007, 2011]. Covariance between *d excess* and latitude is also observed along the same transects (Figure 4).

[44] A simple model of vapor evolution that undergoes Rayleigh distillation modified by recycling of surface water can explain both trends in $\delta^{18}O$ and *d excess* across the plateau (Figure 5, Appendix A, and auxiliary material Table S1). While the relative contribution of unique moisture sources to precipitation may vary across the region and at different altitudes [*Tian et al.*, 2005, 2007], an increased recycled fraction of precipitation inland seems to dominate the isotopic composition of meteoric water on the Tibetan Plateau based on consistent trends in both $\delta^{18}O$ and *d excess* along parallel transects on the eastern and central plateau (Figures 3 and 4b), regardless of variation in air mass mixing (Figures 7a and 7b).

[45] Though the intensity of the Asian monsoon has fluctuated [*Molnar*, 2005; *Sun and Wang*, 2005], the persistence of a proto-Himalaya [*Molnar et al.*, 2010] and proximity of a southern ocean [*Scotese et al.*, 1988; *Ali and Aitchison*, 2008] since the Eocene likely resulted in monsoon circulations [*Boos and Kuang*, 2010]. Thus, recycling of vapor in the rainshadow of the Himalaya should be considered when estimating temporal changes in elevation from isotopes of paleowaters, with the understanding that marine transgressions into the Tarim Basin may disrupt the modern trend. The paleoelevation of the Hoh Xil Basin on the northern Tibetan Plateau is recalculated to account for the modern latitudinal $\delta^{18}O$ gradient, giving a corrected paleoelevation ~1500 m below modern during Eocene-Oligocene time (~3500 m versus ~2040 m from *Cyr et al.* [2005]) and elevations similar to modern in the Miocene. This implies that both the northern and southern Tibetan Plateau were topographically high soon after collision with India, consistent with a model of contemporaneous near and far-field lithospheric deformation [*Dayem et al.*, 2009].

Appendix A: Rayleigh Distillation Modified by Surface Water Recycling

[46] The evolution of $\delta^{18}O$, $\delta^{2}H$, and *d excess* values of both vapor and precipitation are modeled using Rayleigh distillation modified by surface water recycling. Calculations are shown in auxiliary material Table S1. The model starts with a vapor mass of dimensionless size = 1 that experiences six precipitation events where 20% of available vapor condenses as precipitation at each step. 20% is a conservative estimate based on modeling of rainfall to condensation ratios [*Schoenberg Ferrier et al.*, 1996] and measurements of precipitation amount relative to vapor entering a storm [*Fankhauser*, 1988]. Changing the number of precipitation events does not significantly affect model output if the initial and final vapor mass sizes are the same for both cases. We assign the air mass an initial $\delta^{18}O$ value of $-27.7‰$ and $\delta^{2}H$ value of $-209‰$ which produces a first rain with $\delta^{18}O$ of $-18.1‰$ and *d excess* of $\sim 7.6‰$, matching observation on the southern Tibetan Plateau (Figures 3 and 4b). The isotopic composition of reservoir and product phases are calculated using the Rayleigh distillation equation for an air mass undergoing condensation,

$$R = R_o * f^{(\alpha-1)}. \tag{A1}$$

R is defined as $^{18}O/^{16}O$ or $^{2}H/H$ in the residual reservoir, R_o is the initial isotopic ratio of the reservoir before fractionation, f is the fraction remaining, and α is the equilibrium fractionation factor which is empirically defined based on the phase change and temperature [*Majoube*, 1971]. Temperatures of condensation are approximated from the surface dew point (T_d) which is calculated across the plateau using the simple relationship [*Lawrence*, 2005]

$$T_d = T - [(100 - RH)/5]. \tag{A2}$$

[47] According to NCEP/NCAR reanalysis data, mean surface temperatures (T) during summer months (JJA) decrease from ~10°C on the southern plateau to ~5°C on the central plateau, and then increase to ~15°C on its northeast margin [*Kalnay et al.*, 1996]. Relative humidity (RH) decreases monotonically from ~85% to 60% along the same south-north transect (Figure 3). Equation (A1) is in terms of $^{18}O/^{16}O$ ratios (R) so we convert the delta value, which is reported relative to the Vienna Standard Mean Ocean Water standard (VSMOW ~ 0.0020052) using the following equation:

$$\delta^{18}O = \left[\frac{(^{18}O/^{16}O)_{Sample}}{(^{18}O/^{16}O)_{VSMOW}} - 1\right] * 1000. \tag{A3}$$

Table A1. Lake Data Used to Model Rayleigh Distillation of Precipitation Modified by Surface Water Recycling[a]

Lake Name	δ^{18}O (VSMOW)	δ^{2}H (VSMOW)	*d excess*	Latitude	Longitude	Reference
Doqen (Dochen)	−5.1	−50.6	−9.8	28.17	89.35	*Yu et al.* [1984]
Yamzho	−5.3	n/a	n/a	29.13	90.46	*Gao et al.* [2009]
Yamzho	−6.5	−65.5	−13.9	29.13	90.46	*Yu et al.* [1984]
Ngamring	−5.7	−65.5	−20.1	29.3	87.22	*Yu et al.* [1984]
Manasarovar	−3.4	−45.1	−18.3	30.67	81.47	*Yao et al.* [2009]
Unknown	−4.1	−46	−13.2	33.24	88.84	*Hren et al.* [2009]
Unknown	−4	−43	−11	33.91	88.59	*Hren et al.* [2009]
Qinhai	3.5	n/a	n/a	36.91	100.17	*Liu et al.* [2009]

[a]Referred to in section 4.2 and Appendix A.

This gives an initial vapor $^{18}O/^{16}O$ value (R_o) = 0.001949716. Using the Rayleigh distillation equation (A1), we calculate the δ^{18}O value of precipitation. Because we estimate 20% of vapor condenses as rain, f = 0.8. The fractionation factor between vapor and liquid water at 7°C is ∼1.010995868 [*Majoube*, 1971]. Solving equation (A1) for the residual vapor (R) and converting this into delta notation using equation (A3) gives a δ^{18}O value of residual vapor (after 20% is removed as rainfall) of −30.1‰. Based on the δ^{18}O of the vapor before and after precipitation, a mass balance equation is used to calculate the δ^{18}O of precipitation,

$$\delta^{18}O_{original} = (0.2 * \delta^{18}O_{product}) + (0.8 * \delta^{18}O_{residual}). \quad \text{(A4)}$$

[48] After precipitation, we assume surface water evaporates and is integrated into the vapor mass. The isotopic composition of surface water is based on lake water across the Tibetan Plateau (Table A1) where δ^{18}O generally increases from −5‰ on the southern plateau to 3.5‰ in the northeast at Qinhai Lake. Changes in *d excess* are less well-constrained as δ^{2}H data does not exist for many sites. Therefore, we assume a negative *d excess* trend of −5‰ to −15‰ from south to north across the plateau based on evaporation of lake waters under progressively lower relative humidity (Figure 2) [*Gat and Airey*, 2006]. We set the surface water reservoir to be many times larger than the vapor mass and note that changes in reservoir size do not significantly affect isotopic results. The evaporative flux from surface waters is determined by the recycling ratio for each step, defined as the ratio of locally evaporated (on the Tibetan Plateau) to advected vapor (that which arrives from somewhere outside the plateau) in the air mass [*Brubaker et al.*, 1993; *Trenberth*, 1999]. This ratio has been shown to reach 80% on the Tibetan Plateau [*Numaguti*, 1999; *Kurita and Yamada*, 2008]. We assume that vapor entering the plateau already has a recycled fraction of 30% and then increases by 10% for each of the 5 precipitation event thereafter, reaching 80% on the plateau's northern margin.

[49] Though mean surface air temperature across the plateau averages ∼10°C for summer months (JJA) [*Yu et al.*, 2006; *National Oceanic and Atmospheric Administration*, 2010], soil water temperatures during the afternoon are often between 20°C and 30°C [*Yamada and Uyeda*, 2006; *Yang et al.*, 2007b] so we use 20°C as the temperature of surface water evaporation. Because evaporation is occurring at <100% relative humidity (*RH*) (Figure 2), kinetic fractionation is estimated using an equation from *Gonfiantini* [1986]:

$$\Delta\delta^{18}O = 14.2 * (1 - RH). \quad \text{(A5)}$$

[50] Additional calculations of the δ^{18}O of rainfall derived from residual vapor are carried out over five more steps. The δ^{2}H values are calculated using the same boundary conditions. The only differences are the value of VSMOW (^{2}H/H = 0.00015576), the kinetic fractionation equation (A5), and the fractionation factor (α), also based on work by *Majoube* [1971]. Deuterium excess (*d excess*) is also calculated for each precipitation event using equation (1).

Appendix B: Rayleigh Distillation Model for the Himalaya

[51] Calculations are shown in auxiliary material Table S1. The isotopic evolution of precipitation up the windward flank of the Himalaya is modeled using simple Rayleigh distillation (equation (A3)). The only differences are the starting values of δ^{18}O and *d excess* (−8.5‰ and 7.9‰ respectively) which are based on low elevation surface water reported by *Garzione et al.* [2000a], the temperatures of condensation which decrease from 27.5°C to −7°C, and relative humidity, which stays at ∼80%. Temperatures of condensation are estimated from equation (A2) using the mean summer (JJA) surface air temperature (T) at New Delhi (the Himalayan foreland) and at ∼6000 m near Mt. Qomolangma (Everest) which are ∼31.5°C and ∼−3°C respectively [*Xie et al.*, 2006; IAEA/WMO Web site, 2010], and the relative humidity (*RH*) at both sites which is estimated from Figure 2.

[52] **Acknowledgments.** We are grateful to Penny Higgins for assistance with stable isotope lab work at the University of Rochester. We also appreciate moral and logistical support from Alison Duvall and Marin Clark in the field. Last, thank you to three anonymous reviewers whose comments greatly improved the manuscript. This work was supported by NSF grants EAR 0506575 and EAR 0908778 to Garzione, China State Key Laboratory of Earthquake Dynamics grant LED2008A01 to Zhang Peizhen, and an NSEP Boren Fellowship to Bershaw.

References

Aizen, V., E. Aizen, J. Melack, and J. Dozier (1997), Climatic and hydrologic changes in the Tien Shan, central Asia, *J. Clim.*, *10*(6), 1393–1404, doi:10.1175/1520-0442(1997)010<1393:CAHCIT>2.0.CO;2.

Ali, J., and J. Aitchison (2008), Gondwana to Asia: Plate tectonics, paleogeography and the biological connectivity of the Indian sub-continent from the Middle Jurassic through latest Eocene (166–35Ma), *Earth Sci. Rev.*, *88*(3–4), 145–166, doi:10.1016/j.earscirev.2008.01.007.

An, Z., J. Kutzbach, W. Prell, and S. Porter (2001), Evolution of Asian monsoons and phased uplift of the Himalaya—Tibetan plateau since Late Miocene times, *Nature*, *411*(6833), 62–66, doi:10.1038/35075035.

Araguás-Araguás, L., K. Froehlich, and K. Rozanski (1998), Stable isotope composition of precipitation over southeast Asia, *J. Geophys. Res.*, *103*(D22), 28,721–28,742, doi:10.1029/98JD02582.

Barros, A., S. Chiao, T. Lang, D. Burbank, and J. Putkonen (2006), From weather to climate—Seasonal and interannual variability of storms and implications for erosion processes in the Himalaya, *GSA Spec. Pap. 398*, 22 pp., Geol. Soc. of Am., Boulder, Colo.

Boos, W., and Z. Kuang (2010), Dominant control of the South Asian monsoon by orographic insulation versus plateau heating, *Nature*, *463*(7278), 218–222, doi:10.1038/nature08707.

Bosboom, R. E., G. Dupont-Nivet, A. J. P. Houben, H. Brinkhuis, G. Villa, O. Mandic, M. Stoica, W. J. Zachariasse, Z. J. Guo, and C. X. Li (2010), Late Eocene sea retreat from the Tarim Basin (west China) and concomitant Asian paleoenvironmental change, *Palaeogeogr. Palaeoclimatol. Palaeoecol.*, *299*, 385–398, doi:10.1016/j.palaeo.2010.11.019.

Breecker, D., Z. Sharp, and L. McFadden (2009), Seasonal bias in the formation and stable isotopic composition of pedogenic carbonate in modern soils from central New Mexico, USA, *Geol. Soc. Am. Bull.*, *121*(3–4), 630, doi:10.1130/B26413.1.

Breitenbach, S., J. Adkins, H. Meyer, N. Marwan, K. Kumar, and G. Haug (2010), Strong influence of water vapor source dynamics on stable isotopes in precipitation observed in Southern Meghalaya, NE India, *Earth Planet. Sci. Lett.*, *292*(1–2), 212–220, doi:10.1016/j.epsl.2010.01.038.

Brubaker, K., D. Entekhabi, and P. Eagleson (1993), Estimation of continental precipitation recycling, *J. Clim.*, *6*, 1077–1089, doi:10.1175/1520-0442(1993)006<1077:EOCPR>2.0.CO;2.

Buda, A., and D. DeWalle (2009), Using atmospheric chemistry and storm track information to explain the variation of nitrate stable isotopes in precipitation at a site in central Pennsylvania, USA, *Atmos. Environ.*, *43*(29), 4453–4464, doi:10.1016/j.atmosenv.2009.06.027.

Butler, T. J., G. E. Likens, and B. J. B. Stunder (2001), Regional-scale impacts of Phase I of the Clean Air Act Amendments in the USA: The relation between emissions and concentrations, both wet and dry, *Atmos. Environ.*, *35*(6), 1015–1028, doi:10.1016/S1352-2310(00)00386-1.

Chamberlain, C. P., and M. Poage (2000), Reconstructing the paleotopography of mountain belts from the isotopic composition of authigenic minerals, *Geology*, *28*(2), 115, doi:10.1130/0091-7613(2000)28<115:RTPOMB>2.0.CO;2.

Cui, J., S. An, Z. Wang, C. Fang, Y. Liu, H. Yang, Z. Xu, and S. Liu (2009), Using deuterium excess to determine the sources of high-altitude precipitation: Implications in hydrological relations between sub-alpine forests and alpine meadows, *J. Hydrol.*, *373*(1–2), 24–33, doi:10.1016/j.jhydrol.2009.04.005.

Cyr, A., B. Currie, and D. Rowley (2005), Geochemical Evaluation of Fenghuoshan Group Lacustrine Carbonates, North-Central Tibet: Implications for the Paleoaltimetry of the Eocene Tibetan Plateau, *J. Geol.*, *113*, 517–533, doi:10.1086/431907.

Dansgaard, W. (1964), Stable isotopes in precipitation, *Tellus*, *16*(4), 436–468, doi:10.1111/j.2153-3490.1964.tb00181.x.

Dayem, K., P. Molnar, M. Clark, and G. Houseman (2009), Far-field lithospheric deformation in Tibet during continental collision, *Tectonics*, *28*, TC6005, doi:10.1029/2008TC002344.

Dayem, K., P. Molnar, D. Battisti, and G. Roe (2010), Lessons learned from oxygen isotopes in modern precipitation applied to interpretation of speleothem records of paleoclimate from eastern Asia, *Earth Planet. Sci. Lett.*, *295*, 219–230.

Draxler, R. R., and G. D. Hess (1998), An overview of the HYSPLIT_4 modelling system for trajectories, dispersion and deposition, *Aust. Meteorol. Mag.*, *47*(4), 295–308.

Dupont-Nivet, G., W. Krijgsman, C. Langereis, H. Abels, S. Dai, and X. Fang (2007), Tibetan plateau aridification linked to global cooling at the Eocene–Oligocene transition, *Nature*, *445*(7128), 635–638, doi:10.1038/nature05516.

Dupont-Nivet, G., C. Hoorn, and M. Konert (2008), Tibetan uplift prior to the Eocene-Oligocene climate transition: Evidence from pollen analysis of the Xining Basin, *Geology*, *36*(12), 987, doi:10.1130/G25063A.1.

Fankhauser, J. (1988), Estimates of thunderstorm precipitation efficiency from field measurements in CCOPE, *Mon. Weather Rev.*, *116*(3), 663–684, doi:10.1175/1520-0493(1988)116<0663:EOTPEF>2.0.CO;2.

Froehlich, K., J. Gibson, and P. Aggarwal (2002), Deuterium excess in precipitation and its climatological significance, in *Study of Environmental Change Using Isotope Techniques*, *C & S Pap. Ser.*, vol. 13, pp. 54–66, IAEA, Vienna.

Froehlich, K., M. Kralik, W. Papesch, D. Rank, H. Scheifinger, and W. Stichler (2008), Deuterium excess in precipitation of Alpine regions–moisture recycling, *Isotopes Environ. Health Stud.*, *44*(1), 61–70, doi:10.1080/10256010801887208.

Gadgil, S., and K. Rupa Kumar (2006), The Asian monsoon—Agriculture and economy, in *The Asian Monsoon*, edited by B. Wang, pp. 651–683, Springer, New York.

Gao, J., L. Tian, Y. Liu, and T. Gong (2009), Oxygen isotope variation in the water cycle of the Yamzho lake Basin in southern Tibetan Plateau, *Chin. Sci. Bull.*, *54*(16), 2758–2765, doi:10.1007/s11434-009-0487-6.

Garzione, C. N., J. Quade, P. G. DeCelles, and N. B. English (2000a), Predicting paleoelevation of Tibet and the Himalaya from δ^{18}O vs. altitude gradients in meteoric water across the Nepal Himalaya, *Earth Planet. Sci. Lett.*, *183*(1–2), 215–229, doi:10.1016/S0012-821X(00)00252-1.

Garzione, C. N., D. L. Dettman, Q. Jay, P. G. DeCelles, and R. F. Butler (2000b), High times on the Tibetan Plateau; paleoelevation of the Thakkhola Graben, Nepal, *Geology*, *28*(4), 339–342, doi:10.1130/0091-7613(2000)28<339:HTOTTP>2.0.CO;2.

Garzione, C., D. Dettman, and B. Horton (2004), Carbonate oxygen isotope paleoaltimetry: Evaluating the effect of diagenesis on paleoelevation estimates for the Tibetan plateau, *Palaeogeogr. Palaeoclimatol. Palaeoecol.*, *212*(1–2), 119–140.

Garzione, C., M. Ikari, and A. Basu (2005), Source of Oligocene to Pliocene sedimentary rocks in the Linxia basin in northeastern Tibet from Nd isotopes: Implications for tectonic forcing of climate, *Bull. Geol. Soc. Am.*, *117*(9), 1156, doi:10.1130/B25743.1.

Garzione, C. N., P. Molnar, J. C. Libarkin, and B. J. MacFadden (2006), Rapid late Miocene rise of the Bolivian Altiplano: Evidence for removal of mantle lithosphere, *Earth Planet. Sci. Lett.*, *241*(3–4), 543–556, doi:10.1016/j.epsl.2005.11.026.

Gat, J. (1996), Oxygen and hydrogen isotopes in the hydrologic cycle, *Annu. Rev. Earth Planet. Sci.*, *24*(1), 225–262, doi:10.1146/annurev.earth.24.1.225.

Gat, J., and P. Airey (2006), Stable water isotopes in the atmosphere/biosphere/lithosphere interface: Scaling-up from the local to continental scale, under humid and dry conditions, *Global Planet. Change*, *51*(1–2), 25–33, doi:10.1016/j.gloplacha.2005.12.004.

Gat, J., and I. Carmi (1970), Evolution of the isotopic composition of atmospheric waters in the Mediterranean Sea area, *J. Geophys. Res.*, *75*, 3039–3048, doi:10.1029/JC075i015p03039.

Gat, J., A. Shemesh, E. Tziperman, A. Hecht, D. Georgopoulos, and O. Basturk (1996), The stable isotope composition of waters of the eastern Mediterranean Sea, *J. Geophys. Res.*, *101*, 6441–6451, doi:10.1029/95JC02829.

Gile, L., F. Peterson, and R. Grossman (1966), Morphological and genetic sequences of carbonate accumulation in desert soils, *Soil Sci.*, *101*(5), 347, doi:10.1097/00010694-196605000-00001.

Gonfiantini, R. (1986), Environmental isotopes in lake studies, in *Handbook of Environmental Isotope Geochemistry*, edited by P. Fritz and J. C. Fontes, pp. 113–168, Elsevier, New York.

Gonfiantini, R., M. Roche, J. Olivry, J. Fontes, and G. Zuppi (2001), The altitude effect on the isotopic composition of tropical rains, *Chem. Geol.*, *181*(1–4), 147–167, doi:10.1016/S0009-2541(01)00279-0.

Graham, S., C. Chamberlain, Y. Yue, B. Ritts, A. Hanson, T. Horton, J. Waldbauer, M. Poage, and X. Feng (2005), Stable isotope records of Cenozoic climate and topography, Tibetan Plateau and Tarim Basin, *Am. J. Sci.*, *305*(2), 101–118, doi:10.2475/ajs.305.2.101.

Guo, Z., W. Ruddiman, Q. Hao, H. Wu, Y. Qiao, R. Zhu, S. Peng, J. Wei, B. Yuan, and T. Liu (2002), Onset of Asian desertification by 22 Myr ago inferred from loess deposits in China, *Nature*, *416*(6877), 159–163, doi:10.1038/416159a.

Gupta, S., and R. Deshpande (2003), Synoptic hydrology of India from the data of isotopes in precipitation, *Curr. Sci.*, *85*(11), 1591–1595.

Hoke, G., C. Garzione, and L. Chen (2008), Stable isotopic records from Cenozoic basins in the SE Margin of the Tibetan Plateau, Yunnan Province, China: Implications for regional paleoelevation, *Eos Trans. AGU*, *89*(53), Fall Meet Suppl., Abstract T32A-07.

Holdsworth, G., and H. Krouse (2002), Altitudinal variation of the stable isotopes of snow in regions of high relief, *J. Glaciol.*, *48*(160), 31–41, doi:10.3189/172756502781831638.

Horton, B., G. Dupont-Nivet, J. Zhou, G. Waanders, R. Butler, and J. Wang (2004), Mesozoic-Cenozoic evolution of the Xining-Minhe and Dangchang basins, northeastern Tibetan Plateau: Magnetostratigraphic and biostratigraphic results, *J. Geophys. Res.*, *109*, B04402, doi:10.1029/2003JB002913.

Hren, M., B. Bookhagen, P. Blisniuk, A. Booth, and C. Chamberlain (2009), δ^{18}O and δD of streamwaters across the Himalaya and Tibetan Plateau: Implications for moisture sources and paleoelevation reconstructions, *Earth Planet. Sci. Lett.*, *288*, 20–32, doi:10.1016/j.epsl.2009.08.041.

Hsieh, J. C. C., O. A. Chadwick, E. F. Kelly, and S. M. Savin (1998), Oxygen isotopic composition of soil water: Quantifying evaporation and

transpiration, *Geoderma*, *82*(1–3), 269–293, doi:10.1016/S0016-7061(97)00105-5.

Jorba, O., C. Perez, F. Rocadenbosch, and J. M. Baldasano (2004), Cluster analysis of 4-day back trajectories arriving in the Barcelona area, Spain, from 1997 to 2002, *J. Appl. Meteorol.*, *43*(6), 887–901, doi:10.1175/1520-0450(2004)043<0887:CAODBT>2.0.CO;2.

Joswiak, D., T. Yao, G. Wu, B. Xu, and W. Zheng (2010), A 70-yr record of oxygen-18 variability in an ice core from the Tanggula Mountains, central Tibetan Plateau, *Clim. Past*, *6*, 219–227, doi:10.5194/cp-6-219-2010.

Jouzel, J., and L. Merlivat (1984), Deuterium and oxygen 18 in precipitation: Modeling of the isotopic effects during snow formation, *J. Geophys. Res.*, *89*(D7), 11,749–11,757, doi:10.1029/JD089iD07p11749.

Jouzel, J., K. Froehlich, and U. Schotterer (1997), Deuterium and oxygen-18 in present-day precipitation: Data and modelling, *Hydrol. Sci. J.*, *42*(5), 747–763, doi:10.1080/02626669709492070.

Kalnay, E., M. Kanamitsu, R. Kistler, W. Collins, D. Deaven, L. Gandin, M. Iredell, S. Saha, G. White, and J. Woollen (1996), The NCEP/NCAR 40-year reanalysis project, *Bull. Am. Meteorol. Soc.*, *77*(3), 437–471, doi:10.1175/1520-0477(1996)077<0437:TNYRP>2.0.CO;2.

Kang, S., K. Kreutz, P. Mayewski, Q. Dahe, and Y. Tandong (2002), Stable-isotopic composition of precipitation over the northern slope of the central Himalaya, *J. Glaciol.*, *48*(163), 519–526, doi:10.3189/172756502781831070.

Karim, A., and J. Veizer (2002), Water balance of the Indus River Basin and moisture source in the Karakoram and western Himalayas: Implications from hydrogen and oxygen isotopes in river water, *J. Geophys. Res.*, *107*(D18), 4362, doi:10.1029/2000JD000253.

Kendall, C., and T. Coplen (2001), Distribution of oxygen-18 and deuterium in river waters across the United States, *Hydrol. Process.*, *15*(7), 1363–1393, doi:10.1002/hyp.217.

Kent-Corson, M., B. Ritts, G. Zhuang, P. Bovet, S. Graham, and C. Page Chamberlain (2009), Stable isotopic constraints on the tectonic, topographic, and climatic evolution of the northern margin of the Tibetan Plateau, *Earth Planet. Sci. Lett.*, *282*(1–4), 158–166, doi:10.1016/j.epsl.2009.03.011.

Kurita, N., and H. Yamada (2008), The role of local moisture recycling evaluated using stable isotope data from over the middle of the Tibetan Plateau during the monsoon season, *J. Hydrometeorol.*, *9*, 760–775, doi:10.1175/2007JHM945.1.

Kutzbach, J., W. Prell, and W. Ruddiman (1993), Sensitivity of Eurasian climate to surface uplift of the Tibetan Plateau, *J. Geol.*, *101*(2), 177–190, doi:10.1086/648215.

Lawrence, M. (2005), The relationship between relative humidity and the dewpoint temperature in moist air: A simple conversion and applications, *Bull. Am. Meteorol. Soc.*, *86*, 225–233, doi:10.1175/BAMS-86-2-225.

Liotta, M., R. Favara, and M. Valenza (2006), Isotopic composition of the precipitations in the central Mediterranean: Origin marks and orographic precipitation effects, *J. Geophys. Res.*, *111*, D19302, doi:10.1029/2005JD006818.

Liu, W., X. Li, L. Zhang, Z. An, and L. Xu (2009), Evaluation of oxygen isotopes in carbonate as an indicator of lake evolution in arid areas: The modern Qinghai Lake, Qinghai-Tibet Plateau, *Chem. Geol.*, *268*(1–2), 126–136, doi:10.1016/j.chemgeo.2009.08.004.

Majoube, M. (1971), Fractionnement en oxygene-18 et en deuterium entre l'eau et sa vapeur, *J. Chim. Phys.*, *68*, 1423–1436.

Molnar, P. (2005), Mio-Pliocene growth of the Tibetan Plateau and evolution of East Asian climate, *Palaeontol. Electron.*, *8*(1), 2A.

Molnar, P., W. Boos, and D. Battisti (2010), Orographic controls on climate and paleoclimate of Asia: Thermal and mechanical roles for the Tibetan Plateau, *Annu. Rev. Earth Planet. Sci.*, *38*, 77–102, doi:10.1146/annurev-earth-040809-152456.

Mulch, A., C. E. Uba, M. R. Strecker, R. Schoenberg, and C. P. Chamberlain (2010), Late Miocene climate variability and surface elevation in the central Andes, *Earth Planet. Sci. Lett.*, *290*(1–2), 173–182, doi:10.1016/j.epsl.2009.12.019.

National Oceanic and Atmospheric Administration (2010), NCEP/NCAR reanalysis data, http://www.esrl.noaa.gov/psd/data/gridded/reanalysis/, ESRL Phys. Sci. Div., NOAA, Boulder, Colo.

Numaguti, A. (1999), Origin and recycling processes of precipitating water over the Eurasian continent: Experiments using an atmospheric general circulation model, *J. Geophys. Res.*, *104*(D2), 1957–1972, doi:10.1029/1998JD200026.

Pang, Z., Y. Kong, K. Froehlich, T. Huang, L. Yuan, Z. Li, and F. Wang (2011), Processes affecting isotopes in precipitation of an arid region, *Tellus, Ser. B*, *63*, 352–359.

Peng, T., C. Wang, C. Huang, L. Fei, C. Chen, and J. Hwong (2009), Stable isotopic characteristic of Taiwan's precipitation: A case study of western Pacific monsoon region, *Earth Planet. Sci. Lett.*, *289*(3–4), 357–366.

Petit, J., J. White, N. Young, J. Jouzel, and Y. Korotkevich (1991), Deuterium excess in recent Antarctic snow, *J. Geophys. Res.*, *96*(D3), 5113–5122, doi:10.1029/90JD02232.

Poage, M. A., and C. P. Chamberlain (2001), Empirical relationships between elevation and the stable isotope composition of precipitation and surface waters; considerations for studies of paleoelevation change, *Am. J. Sci.*, *301*(1), 1–15, doi:10.2475/ajs.301.1.1.

Polissar, P. J., K. H. Freeman, D. B. Rowley, F. A. McInerney, and B. S. Currie (2009), Paleoaltimetry of the Tibetan Plateau from D/H ratios of lipid biomarkers, *Earth Planet. Sci. Lett.*, *287*(1–2), 64–76, doi:10.1016/j.epsl.2009.07.037.

Quade, J., C. N. Garzione, and J. Eiler (2007), Paleoelevation reconstruction using pedogenic carbonates, *Rev. Mineral. Geochem.*, *66*(1), 53–87, doi:10.2138/rmg.2007.66.3.

Quade, J., D. O. Breecker, M. Daeron, and J. Eiler (2011), The paleoaltimetry of Tibet: An isotopic perspective, *Am. J. Sci.*, *311*(2), 77–115, doi:10.2475/02.2011.01.

Ramstein, G., F. Fluteau, J. Besse, and S. Joussaume (1997), Effect of orogeny, plate motion and land-sea distribution on Eurasian climate change over the past 30 million years, *Nature*, *386*, 788–795, doi:10.1038/386788a0.

Ritts, B., Y. Yue, and S. Graham (2004), Oligocene-Miocene tectonics and sedimentation along the Altyn Tagh Fault, Northern Tibetan Plateau: Analysis of the Xorkol, Subei, and Aksay Basins, *J. Geol.*, *112*, 207–229, doi:10.1086/381658.

Ritts, B., Y. Yue, S. Graham, E. Sobel, O. Abbink, and D. Stockli (2008), From sea level to high elevation in 15 million years: Uplift history of the northern Tibetan Plateau margin in the Altun Shan, *Am. J. Sci.*, *308*(5), 657–678, doi:10.2475/05.2008.01.

Rowley, D. (1996), Age of initiation of collision between India and Asia: A review of stratigraphic data, *Earth Planet. Sci. Lett.*, *145*(1–4), 1–13, doi:10.1016/S0012-821X(96)00201-4.

Rowley, D., and C. Garzione (2007), Stable isotope-based paleoaltimetry, *Annu. Rev. Earth Planet. Sci.*, *35*, 463–508, doi:10.1146/annurev.earth.35.031306.140155.

Rowley, D. B., R. T. Pierrehumbert, and B. S. Currie (2001), A new approach to stable isotope-based paleoaltimetry: Implications for paleoaltimetry and paleohypsometry of the High Himalaya since the Late Miocene, *Earth Planet. Sci. Lett.*, *188*(1–2), 253–268, doi:10.1016/S0012-821X(01)00324-7.

Rozanski, K., L. Araguás-Araguás, and R. Gonfiantini (1993), Isotopic patterns in modern global precipitation, in *Climate Change in Continental Isotopic Records*, *Geophys. Monogr. Ser.*, vol. 78, edited by P. K. Swart et al., pp. 1–36, AGU, Washington, D. C., doi:10.1029/GM078p0001.

Salati, E., A. Dall'Olio, E. Matsui, and J. Gat (1979), Recycling of water in the Amazon basin: An isotopic study, *Water Resour. Res.*, *15*(5), 1250–1258, doi:10.1029/WR015i005p01250.

Saylor, J. E., J. Quade, D. L. Dettman, P. G. DeCelles, P. A. Kapp, and L. Ding (2009), The late Miocene through present paleoelevation history of southwestern Tibet, *Am. J. Sci.*, *309*(1), 1, doi:10.2475/01.2009.01.

Schoenberg Ferrier, B., J. Simpson, and W. Tao (1996), Factors responsible for precipitation efficiencies in midlatitude and tropical squall simulations, *Mon. Weather Rev.*, *124*(10), 2100–2125, doi:10.1175/1520-0493(1996)124<2100:FRFPEI>2.0.CO;2.

Scholl, M., T. Giambelluca, S. Gingerich, M. Nullet, and L. Loope (2007), Cloud water in windward and leeward mountain forests: The stable isotope signature of orographic cloud water, *Water Resour. Res.*, *43*, W12411, doi:10.1029/2007WR006011.

Scotese, C., L. Gahagan, and R. Larson (1988), Plate tectonic reconstructions of the Cretaceous and Cenozoic ocean basins, *Tectonophysics*, *155*(1–4), 27–48, doi:10.1016/0040-1951(88)90259-4.

Searle, M., R. Corfield, B. Stephenson, and J. McCarron (1997), Structure of the North Indian continental margin in the Ladakh–Zanskar Himalayas: Implications for the timing of obduction of the Spontang ophiolite, India—Asia collision and deformation events in the Himalaya, *Geol. Mag.*, *134*(3), 297–316, doi:10.1017/S0016756897006857.

Sjostrom, D., and J. Welker (2009), The influence of air mass source on the seasonal isotopic composition of precipitation, eastern USA, *J. Geochem. Explor.*, *102*(3), 103–112, doi:10.1016/j.gexplo.2009.03.001.

Spicer, R., N. Harris, M. Widdowson, A. Herman, S. Guo, P. Valdes, J. Wolfe, and S. Kelley (2003), Constant elevation of southern Tibet over the past 15 million years, *Nature*, *421*(6923), 622–624, doi:10.1038/nature01356.

Stewart, M. (1975), Stable isotope fractionation due to evaporation and isotopic exchange of falling waterdrops: Applications to atmospheric processes and evaporation of lakes, *J. Geophys. Res.*, *80*(9), 1133–1146, doi:10.1029/JC080i009p01133.

Sun, J., J. Ye, W. Wu, X. Ni, S. Bi, Z. Zhang, W. Liu, and J. Meng (2010), Late Oligocene–Miocene mid-latitude aridification and wind patterns in the Asian interior, *Geology*, *38*(6), 515–518, doi:10.1130/G30776.1.

Sun, X., and P. Wang (2005), How old is the Asian monsoon system?—Palaeobotanical records from China, *Palaeogeogr. Palaeoclimatol. Palaeoecol.*, *222*(3–4), 181–222, doi:10.1016/j.palaeo.2005.03.005.

Tao, F., M. Yokozawa, Z. Zhang, Y. Hayashi, H. Grassl, and C. Fu (2004), Variability in climatology and agricultural production in China in association with the East Asian summer monsoon and El Niño Southern Oscillation, *Clim. Res.*, *28*, 23–30, doi:10.3354/cr028023.

Thompson, L., T. Yao, E. Mosley-Thompson, M. Davis, K. Henderson, and P. Lin (2000), A high-resolution millennial record of the South Asian monsoon from Himalayan ice cores, *Science*, *289*(5486), 1916–1919, doi:10.1126/science.289.5486.1916.

Tian, L., V. Masson-Delmotte, M. Stievenard, T. Yao, and J. Jouzel (2001), Tibetan Plateau summer monsoon northward extent revealed by measurements of water stable isotopes, *J. Geophys. Res.*, *106*(D22), 28,081–28,088, doi:10.1029/2001JD900186.

Tian, L., Y. Tandong, J. White, Y. Wusheng, and W. Ninglian (2005), Westerly moisture transport to the middle of Himalayas revealed from the high deuterium excess, *Chin. Sci. Bull.*, *50*(10), 1026–1030, doi:10.1360/04wd0030.

Tian, L., T. Yao, K. MacClune, J. W. C. White, A. Schilla, B. Vaughn, R. Vachon, and K. Ichiyanagi (2007), Stable isotopic variations in west China: A consideration of moisture sources, *J. Geophys. Res.*, *112*, D10112, doi:10.1029/2006JD007718.

Trenberth, K. (1999), Atmospheric moisture recycling: Role of advection and local evaporation, *J. Clim.*, *12*, 1368–1381, doi:10.1175/1520-0442(1999)012<1368:AMRROA>2.0.CO;2.

Tsujimura, M., A. Numaguti, L. Tian, S. Hashimoto, A. Sugimoto, and M. Nakawo (2001), Behavior of subsurface water revealed by stable isotope and tensiometric observation in the Tibetan Plateau, *J. Meteorol. Soc. Jpn.*, *79*(1B), 599–605, doi:10.2151/jmsj.79.599.

Ueno, K., H. Fujii, H. Yamada, and L. Liu (2001), Weak and frequent monsoon precipitation over the Tibetan Plateau, *J. Meteorol. Soc. Jpn.*, *79*(1B), 419–434, doi:10.2151/jmsj.79.419.

Vuille, M., M. Werner, R. Bradley, and F. Keimig (2005), Stable isotopes in precipitation in the Asian monsoon region, *J. Geophys. Res.*, *110*, D23108, doi:10.1029/2005JD006022.

Wallace, J., and P. Hobbs (2006), *Atmospheric Science: An Introductory Survey*, Academic, San Diego, Calif.

Wang, J., Y. Wang, Z. Liu, J. Li, and P. Xi (1999), Cenozoic environmental evolution of the Qaidam Basin and its implications for the uplift of the Tibetan Plateau and the drying of central Asia, *Palaeogeogr. Palaeoclimatol. Palaeoecol.*, *152*(1–2), 37–47, doi:10.1016/S0031-0182(99)00038-3.

Wang, Q., T. Nishidai, and M. Coward (1992), The Tarim Basin, NW China: Formation and aspects of petroleum geology, *J. Pet. Geol.*, *15*(1), 5–34, doi:10.1111/j.1747-5457.1992.tb00863.x.

Wen, L., P. Cui, Y. Li, C. Wang, Y. Liu, N. Chen, and F. Su (2010), The influence of sensible heat on monsoon precipitation in central and eastern Tibet, *Meteorol. Appl.*, *17*, 452–462, doi:10.1002/met.181.

Xie, A., J. Ren, X. Qin, and Y. Jiang (2006), Meteorological features at 6523 m of Mt. Qomolangma (Everest) between 1 May and 22 July 2005, *J. Mt. Sci.*, *3*(3), 181–190, doi:10.1007/s11629-006-0181-y.

Yamada, H., and H. Uyeda (2006), Transition of the rainfall characteristics related to the moistening of the land surface over the central Tibetan Plateau during the summer of 1998, *Mon. Weather Rev.*, *134*, 3230–3247, doi:10.1175/MWR3235.1.

Yanai, M., and G. Wu (2006), Effects of the Tibetan Plateau, in *The Asian Monsoon*, edited by B. Wang, pp. 513–549, Springer, New York.

Yang, M., T. Yao, H. Wang, L. Tian, and X. Gou (2006), Estimating the criterion for determining water vapour sources of summer precipitation on the northern Tibetan Plateau, *Hydrol. Process.*, *20*(3), 505–513, doi:10.1002/hyp.5918.

Yang, M., T. Yao, X. Gou, and H. Tang (2007a), Water recycling between the land surface and atmosphere on the Northern Tibetan Plateau—A case study at flat observation sites, *Arct. Antarct. Alp. Res.*, *39*(4), 694–698, doi:10.1657/1523-0430(07–509)[YANG]2.0.CO;2.

Yang, M., T. Yao, X. Gou, N. Hirose, H. Fujii, L. Hao, and D. Levia (2007b), Diurnal freeze/thaw cycles of the ground surface on the Tibetan Plateau, *Chin. Sci. Bull.*, *52*(1), 136–139, doi:10.1007/s11434-007-0004-8.

Yao, Z., J. Liu, H. Huang, X. Song, X. Dong, and X. Liu (2009), Characteristics of isotope in precipitation, river water and lake water in the Manasarovar basin of Qinghai– Tibet Plateau, *Environ. Geol.*, *57*(3), 551–556, doi:10.1007/s00254-008-1324-y.

Yin, A., P. Rumelhart, R. Butler, E. Cowgill, T. Harrison, D. Foster, R. Ingersoll, Z. Qing, Z. Xian-Qiang, and W. Xiao-Feng (2002), Tectonic history of the Altyn Tagh fault system in northern Tibet inferred from Cenozoic sedimentation, *Geol. Soc. Am. Bull.*, *114*(10), 1257, doi:10.1130/0016-7606(2002)114<1257:THOTAT>2.0.CO;2.

Yin, A., Y. Dang, M. Zhang, X. Chen, and M. McRivette (2008), Cenozoic tectonic evolution of the Qaidam basin and its surrounding regions (Part 3), Structural geology, sedimentation, and regional tectonic reconstruction, *Geol. Soc. Am. Bull.*, *120*(7–8), 847, doi:10.1130/B26232.1.

Yu, J., H. Zhang, F. Yu, and D. Liu (1984), Oxygen and hydrogen isotopic compositions of meteoric waters in the eastern part of Xizang, *Chin. J. Geochem.*, *3*(2), 93–101.

Yu, W., T. Yao, L. Tian, Y. Wang, Z. Li, and W. Sun (2006), Oxygen-18 isotopes in precipitation on the eastern Tibetan Plateau, *Ann. Glaciol.*, *43*(1), 263–268, doi:10.3189/172756406781812447.

Yu, W., T. Yao, L. Tian, Y. Ma, N. Kurita, K. Ichiyanagi, Y. Wang, and W. Sun (2007), Stable isotope variations in precipitation and moisture trajectories on the western Tibetan Plateau, China, *Arct. Antarct. Alp. Res.*, *39*(4), 688–693, doi:10.1657/1523-0430(07–511)[YU]2.0.CO;2.

Yu, W., T. Yao, L. Tian, Y. Ma, K. Ichiyanagi, Y. Wang, and W. Sun (2008), Relationships between $\delta^{18}O$ in precipitation and air temperature and moisture origin on a south-north transect of the Tibetan Plateau, *Atmos. Res.*, *87*(2), 158–169, doi:10.1016/j.atmosres.2007.08.004.

Zachos, J., L. Stott, and K. Lohmann (1994), Evolution of early Cenozoic marine temperatures, *Paleoceanography*, *9*, 353–387, doi:10.1029/93PA03266.

Zachos, J., M. Pagani, L. Sloan, E. Thomas, and K. Billups (2001), Trends, rhythms, and aberrations in global climate 65 Ma to present, *Science*, *292*(5517), 686–693, doi:10.1126/science.1059412.

Zhang, Z., H. Wang, Z. Guo, and D. Jiang (2007), What triggers the transition of palaeoenvironmental patterns in China, the Tibetan Plateau uplift or the Paratethys Sea retreat?, *Palaeogeogr. Palaeoclimatol. Palaeoecol.*, *245*(3–4), 317–331.

Zhou, J., F. Xu, T. Wang, A. Cao, and C. Yin (2006), Cenozoic deformation history of the Qaidam Basin, NW China: Results from cross-section restoration and implications for Qinghai-Tibet Plateau tectonics, *Earth Planet. Sci. Lett.*, *243*(1–2), 195–210, doi:10.1016/j.epsl.2005.11.033.

Zhu, B., W. Kidd, D. Rowley, B. Currie, and N. Shafique (2005), Age of initiation of the India-Asia collision in the East-Central Himalaya, *J. Geol.*, *113*, 265–285, doi:10.1086/428805.

Zhu, L., C. Wang, H. Zheng, F. Xiang, H. Yi, and D. Liu (2006), Tectonic and sedimentary evolution of basins in the northeast of Qinghai-Tibet Plateau and their implication for the northward growth of the plateau, *Palaeogeogr. Palaeoclimatol. Palaeoecol.*, *241*(1), 49–60, doi:10.1016/j.palaeo.2006.06.019.

Zunckel, M., C. Saizar, and J. Zarauz (2003), Rainwater composition in northeast Uruguay, *Atmos. Environ.*, *37*(12), 1601–1611, doi:10.1016/S1352-2310(03)00007-4.

J. Bershaw and C. N. Garzione, Department of Earth and Environmental Sciences, University of Rochester, 227 Hutchison Hall, Rochester, NY 14627, USA. (jbershaw@gmail.com)

S. M. Penny, Department of Atmospheric Sciences, University of Washington, 408 ATG Bldg., Box 351640, Seattle, WA 98195-1640, USA.